STABILITY AND BIFURCATION OF AUTONOMOUS VEHICLES IN THE PRESENCE OF POSITIONAL INFORMATION TIME LAGS

by

George P. Cummings
Lieutenant Commander, United States Coast Guard
B.S., United States Coast Guard Academy, 1982

Submitted in partial fulfillment
of the requirements for the degree of

MASTER'S OF SCIENCE IN MECHANICAL ENGINEERING

from the

REPORT DOCUMENTATION PAGE

Form Approved OMB No. 0704

1. AGENCY USE ONLY	2. REPORT DATE 23 September 1993	3. REPORT TYPE AND DATES COVERED Master's Thesis

4. TITLE AND SUBTITLE STABILITY AND BIFURCATION OF AUTONOMOUS VEHICLES IN THE PRESENCE OF POSITIONAL INFORMATION TIME LAGS	5. FUNDING NUMBERS
6. AUTHOR(S) *CUMMINGS, George Patrick*	
7. PERFORMING ORGANIZATION NAME(S) AND ADDRESS(ES) Naval Postgraduate School Monterey, CA 93943-5000	8. PERFORMING ORGANIZATION REPORT NUMBER
9. SPONSORING/MONITORING AGENCY NAME(S) AND ADDRESS(ES)	10. SPONSORING/MONITORING AGENCY REPORT NUMBER

11. SUPPLEMENTARY NOTES The views expressed in this thesis are those of the author and do not reflect the official policy or position of the Department of Defense or the U.S. Government.

12a. DISTRIBUTION/AVAILABILITY STATEMENT Approved for public release; distribution is unlimited.	12b. DISTRIBUTION CODE *A

13.

ABSTRACT

The track keeping characteristics of an autonomous ocean vehicle in the presence of a realistic time lag on the vehicle's position information is examined in two ways. A Hopf bifurcation analysis is applied to better predict vehicle behavior within its region of linearized classical stability. Additionally, the effects on guidance /control stability by the use of a single stage memory model incorporating the two previous vehicle positions in place of a single position data point is investigated. Results are presented using a dynamic model of the Naval Postgraduate School Autonomous Underwater Vehicle II (NPS AUV).

14. SUBJECT TERMS	15. NUMBER OF PAGES 80
	16. PRICE CODE

17. SECURITY CLASSIFICATION OF REPORT Unclassified	18. SECURITY CLASSIFICATION OF THIS PAGE Unclassified	19. SECURITY CLASSIFICATION OF ABSTRACT Unclassified	20. LIMITATION OF ABSTRACT UL

NSN 7540-01-280-5500

Standard Form 298 (Rev. 2-89)
Prescribed by ANSI STD. 239-18

ABSTRACT

The track keeping characteristics of an autonomous ocean vehicle in the presence of a realistic time lag on the vehicle's positional information is examined in two ways. A Hopf bifurcation analysis is applied to better predict vehicle behavior within its region of linearized classical stability. Additionally, the effects on guidance/control stability by the use of a single stage memory model incorporating the two previous position data points in place of a single position data point is investigated. Results are presented using a dynamic model of the Naval Postgraduate School Autonomous Underwater Vehicle II (NPS AUV II).

TABLE OF CONTENTS

I. INTRODUCTION

A. BACKGROUND

Autonomous vehicles suitable for use in modern applications require high maneuverability, quick response, and robust performance characteristics [Ref. 7]. In order to maintain accurate track keeping characteristics, a suitable combination of path planning, navigation, guidance, and control design is needed [Ref. 10]. Sufficient information is obtained from charted obstacles and the environment for smooth paths to be generated for the vehicle to follow [Ref. 8]. Although it is possible to design a nonlinear controller which incorporates and utilizes information on the nonlinear dynamic properties of the vehicle, as well as the geometric nonlinearities of the desired track, the resulting scheme tends to be very complex and time consuming [Ref. 3]. The alternative is to use separated navigation, guidance, and autopilot functions. A certain level of feedback is provided at the navigation level through the use of sonars in order to replan a path due to uncharted obstacles or changes in mission objectives. This operation is event-driven and occurs asynchronously, and in many cases it does not affect stability and performance of the overall navigation, guidance, and control scheme. Based on the provided navigational

information, the guidance law generates heading commands, which are executed by the control law by appropriate use of vehicle effectors, such as control surfaces and cross body thrusters. However, the time required to process sonar data and/or inertial position information may be significant and cannot be neglected [Ref. 9]. In addition, the guidance and control laws must be as fast as possible in order to ensure accurate path keeping characteristics. The navigational position information time lags, as well as the dynamic lags due to the vehicle inertia, however, set a limit on the vehicle reaction time. Therefore, stability of the combined scheme becomes an issue which requires analysis.

B. OBJECTIVE

Previous studies have established boundaries for guidance and control laws in the horizontal [Ref. 10] and vertical plane [Ref. 12] maneuvering along straight line paths, as well as curved segments [Ref. 11]. The most important assumption in those results was the existence of instantaneous positional information updates when needed. In this work we relax the latter assumption. Stability boundaries are computed parametrized by the amount of positional information time lag. Results are presented based on eigenvalue and frequency response techniques. This thesis builds on the linear stability analysis performed in [Ref. 13] which can predict the shape of the stability boundaries. In this work, vehicle

motions in the vicinity of the corresponding boundary are assessed using nonlinear bifurcation theory [Ref. 5]. It is shown that the loss of stability occurs as generic Hopf bifurcations, where upon loss of stability of straight line motion a family of periodic solutions appears. Nonlinear expansions utilizing center manifold approximations and integral averaging techniques, reveal that these Hopf bifurcations can occur either in supercritical or subcritical forms. In the supercritical case, a stable family of limit cycles is generated immediately after the nominal motion becomes unstable. In the subcritical case, however, the resulting limit cycles are initially unstable and they are generated even before the nominal motion loses its stability. In the latter case, the domain of convergence of straight line motion becomes increasingly smaller as the stability boundary is reached. As a result, the methods developed in this work characterize the degree of confidence of the computed stability boundaries by examining stability under finite external disturbances. A first order memory scheme, which can be easily implemented in real time, is suggested in order to expand the region of stability of straight line motion. All computations are performed for the NPS autonomous underwater vehicle for which a set of geometric properties and slow motion hydrodynamic derivatives is available [Ref. 1]. Unless otherwise mentioned, all results are presented in standard nondimensional form. Equation development presented in

[Ref.13] has been used in chapter II, and with modifications in chapter IV.

C. THESIS OUTLINE

Chapter II presents the formulation of vehicle equations of motion and the criterion for determining the region of guidance/control stability in the presence of a position information time lag.

Chapter III examines the vehicle's control stability through the use of a Hopf bifurcation analysis.

Chapter IV examines the effect on the region of stability determination by the use of a memory model which incorporates the two previous vehicle positions.

II. PROBLEM FORMULATION

A. EQUATIONS OF MOTION

The mathematical model which describes vehicle motion in the horizontal plane consists of nonlinear sway and yaw equations of motion. A moving coordinate frame which is fixed at the vehicle's geometric center gives Newtonian equations of motion which are

$$m(\dot{v}+ur+x_G\dot{r}-y_Gr^2)=Y \qquad (2.1)$$

$$I_Z\dot{r}+mx_G(\dot{v}+ur)-my_Gvr=N \qquad (2.2)$$

where u is constant forward speed; v and r are the relative sway and yaw velocities of the moving vehicle relative to the water; m is the mass of the moving vehicle; x_G, y_G are the respective lateral and longitudinal positions of the center of gravity; and Y, N represent the total excitation sway force and yaw moment, respectively. The vehicle's added mass, damping, and viscous drag due to motion through the water are represented by quadratic drag terms and memoryless polynomials in v and r. Y and N can be represented as the sum of these terms by

$$Y=\frac{\rho}{2}l^4Y_{\dot r}\dot r+\frac{\rho}{2}l^3(Y_{\dot v}\dot v+Y_r ur)+\frac{\rho}{2}l^2Y_v uv$$
$$-\frac{\rho}{2}\int_{tail}^{nose}C_{D_y}h(\xi)\frac{(v+\xi r)^3}{|v+\xi r|}\xi d\xi+\frac{\rho}{2}l^2Y_\delta u^2\delta$$

$$N=\frac{\rho}{2}l^5N_{\dot r}\dot r+\frac{\rho}{2}l^4(N_{\dot v}\dot v+N_r ur)+\frac{\rho}{2}l^3N_v uv$$
$$-\frac{\rho}{2}\int_{tail}^{nose}C_{D_y}h(\xi)\frac{(v+\xi r)^3}{|v+\xi r|}\xi d\xi+\frac{\rho}{2}l^3N_\delta u^2\delta$$

where l is the vehicle length, Y_a, N_a represent partial derivatives of Y and N with respect to a, C_{Dy} is the drag coefficient, and δ is the rudder angle.

At relatively high speeds and low angles of attack the steering response is predominantly linear. In low speed maneuvering or hovering conditions the cross flow integral drag term becomes significant.

Vehicle yaw rate is expressed by

$$\psi=r \tag{2.3}$$

and inertial position rate is expressed by

$$\dot y=u\sin\psi+v\cos\psi \tag{2.4}$$

where ψ is the heading angle and shown in Figure 1.

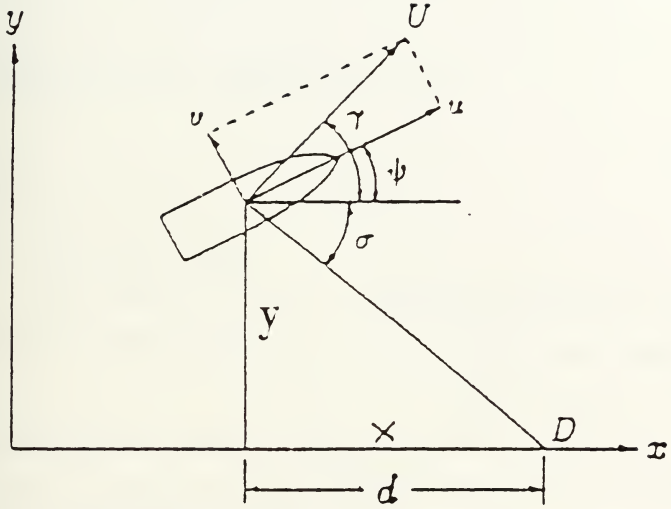

Figure 1. Vehicle Geometry and Definition of Symbols.

Taking equations (2.1), (2.2), and (2.3) as a set of three coupled linear differential equations, and a linearized form of equation (2.4), the final set of equations of motion for steering control are

$$\psi = r \tag{2.5a}$$

$$\dot{v} = a_{11}uv + a_{12}ur + b_1 u^2 \delta \tag{2.5b}$$

$$\dot{r} = a_{21}uv + a_{22}ur + b_2 u^2 \delta \tag{2.5c}$$

$$\dot{y} = u\psi + v \tag{2.5d}$$

at any nominal forward speed.

B. GUIDANCE AND CONTROL

1. Guidance Scheme

An orientation based command scheme is used where the commanded vehicle heading angle ψ_c is a function of the line of sight angle σ between the actual vehicle position and a reference position on the nominal path located at a constant lookahead distance d. Schematically, this is presented in Figure 1.

The line of sight angle σ is defined by

$$\tan\sigma = -\frac{y}{d} \tag{2.6}$$

The autopilot will be called upon to orient the vehicle to the commanded heading angle ψ_c, which, in pursuit guidance, will equal the line of sight angle. This defines ψ_c as

$$\psi_c = -\arctan\frac{y}{d} \tag{2.7}$$

For relatively small angles

$$\psi_c \approx -\frac{y}{d} \tag{2.8}$$

2. Controller Design

The steering control governing equations can be represented in the form

$$\dot{x} = Ax + b\delta \tag{2.9}$$

where the state vector equation is

$$x = [\psi, v, r]^T \tag{2.10}$$

Linear full state feedback is introduced in the form

$$\delta = k_1(\psi - \psi_c) + k_2 v + k_3 r \qquad (2.11)$$

The gains k_1, k_2, and k_3 are computed by pole placement to give the desired dynamics to the closed loop system. The vehicle's longitudinal axis is pointed toward the desired heading by the difference $(\psi - \psi_c)$ in the control law.

With a dimensionless time constant t_c the general form of the characteristic equation is

$$\lambda^3 + \alpha_1 \lambda^2 + \alpha_2 \lambda + \alpha_3 = 0 \qquad (2.12)$$

where

$$\alpha_1 = \frac{3}{t_c},\ \alpha_2 = \frac{3}{t^2},\ \alpha_3 = \frac{1}{t^3}$$

The controller gains are computed from

$$k_1 = \frac{\alpha_3}{(b_2 a_{11} - b_1 a_{21}) u^3} \qquad (2.13a)$$

$$\begin{aligned}(b_1 a_{22} - b_2 a_{12}) u^3 k_2 + (b_2 a_{11} - b_1 a_{21}) u^3 k_3 \\ = \alpha_2 + b_2 u^2 k_1 - (a_{11} a_{22} - a_{12} a_{21}) u^2\end{aligned} \qquad (2.13b)$$

$$b_1 u^2 k_2 + b_2 u^2 k_3 = -\alpha_1 - (a_{11} + a_{22}) u \qquad (2.13c)$$

These gain values are continuously updated due to changing nominal forward speeds. Figure 2 shows the three controller gains at unit forward speed versus the system time constant.

C. TIME LAG

All of the required state information for vehicle control is available at sufficient rates with the possible exception of the y position information. Due to time requirements for reduction of sonar returns and inertial navigation information, there may be a time lag in the y position information.

This time lag T (sec) is introduced to the guidance control law and the commanded rudder angle ψ_c becomes

$$\psi_c = -\arctan \frac{y(t-T)}{d} \tag{2.14}$$

For small angles

$$\psi_c \approx -\frac{y(t-T)}{d} \tag{2.15}$$

and the resulting linearized control law becomes

$$\delta = k_1 \psi + k_1 \frac{y(t-T)}{d} + k_2 v + k_3 r \tag{2.16}$$

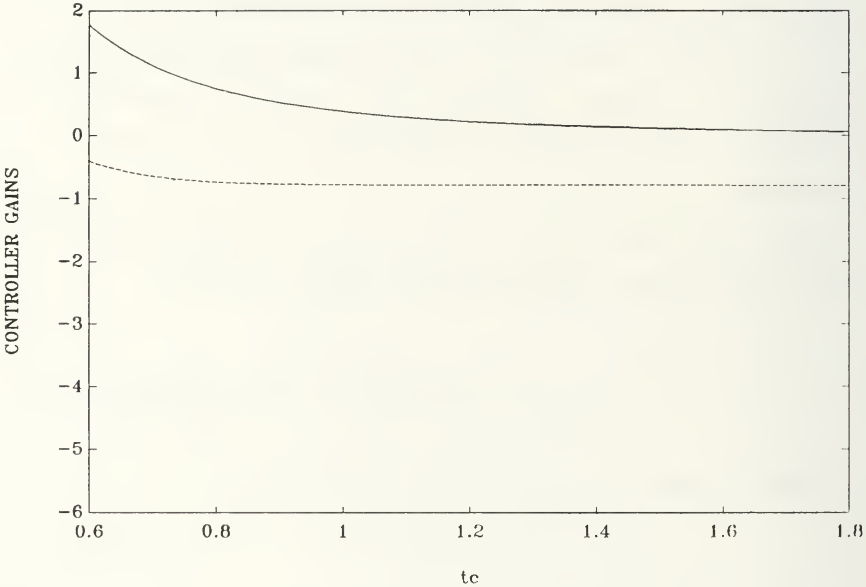

Figure 2. Controller Gains versus t_c at unit forward speed. (k_1=solid, k_2=dashed, k_3=dotted)

The linearized equations of motion become

$$\psi = r \tag{2.17a}$$

$$\begin{aligned}\dot{v} &= b_1 u^2 k_1 \psi + (a_{11} u + b_1 u^2 k_2) v \\ &+ (a_{12} u + b_1 u^2 k_3) r + b_1 u^2 \frac{k_1}{d} y(t-T)\end{aligned} \tag{2.17b}$$

$$\begin{aligned}\dot{r} &= b_2 u^2 k_1 \psi + (a_{21} u + b_2 u^2 k_2) v \\ &+ (a_{22} u + b_2 u^2 k_3) r + b_2 u^2 \frac{k_1}{d} y(t-T)\end{aligned} \tag{2.17c}$$

$$\dot{y} = u\psi + v \tag{2.17d}$$

D. STABILITY ANALYSIS

Control law stability is determined by the eigenvalues of the matrix **A** from the linear system

$$\dot{x} = Ax \tag{2.18}$$

with the state vector

$$x = [\psi, v, r, y]^T \tag{2.19}$$

where the state equations have been linearized around straight line motion. The characteristic equation of (2.18) is a quartic of the form

$$\lambda^4+B\lambda^3+C\lambda^2+D\lambda+E=0 \tag{2.20}$$

where the coefficients B, C, D, and E are functions of vehicle properties, controller gains, and lookahead distance.

The characteristic equation will give a pair of complex conjugate roots which cross the imaginary axis under the following conditions.

$$BCD-B^2E-D^2=0 \tag{2.21a}$$

$$\frac{D}{B}>0 \tag{2.21b}$$

Minimum lookahead distance d_{crit} for stability can be determined by translating these conditions to

$$a_1d^2+a_2d+a_3=0 \tag{2.22a}$$

$$d>\frac{b_1a_{22}-b_2a_{12}-b_2}{b_2a_{11}-b_1a_{21}} \tag{2.22b}$$

where

$$a_1 = \alpha_1\alpha_2 - \alpha_3 \tag{2.23a}$$

$$a_2 = \frac{(\alpha_1\alpha_2 - 2\alpha_3)(b_1a_{22} - b_2a_{12} - b_2)}{b_2a_{11} - b_1a_{21}} - \frac{b_1\alpha_1\alpha_3}{(b_2a_{11} - b_1a_{21})u} - \alpha^2 u \tag{2.23b}$$

$$a_3 = \frac{-(b_1a_{22} - b_2a_{12} - b_2)[b_1\alpha_1 + (b_1a_{22} - b_2a_{12} - b_2)u]\alpha_3}{(b_2a_{11} - b_1a_{21})^2 u} \tag{2.23c}$$

Analysis of the system when operating with an information time lag requires approximation by either a first order Taylor expansion

$$y(t-T) \doteq y - T\dot{y} \tag{2.24}$$

a second order Taylor expansion

$$y(t-T) \doteq y - T\dot{y} + \frac{T^2}{2}\ddot{y} \tag{2.25}$$

a third order Taylor expansion

$$y(t-T) \doteq y - T\dot{y} + \frac{T^2}{2}\ddot{y} - \frac{T^3}{6}\dddot{y} \tag{2.26}$$

or a frequency response analysis using the Nyquist criterion. Figure 3 shows the region of stability given by each of these

methods with a one second (dimentionless) time lag. It can be seen that the agreement is, in general, very good among the three Taylor series approximations, especially as the time constant t_c is increased. The third order approximation coincides with the exact solution from the frequency response (Nyquist criterion) method. The first order method requires the highest value of d for stability at a given t_c, and therefore is the most conservative method for design use. For this reason the first order method is used in the next chapter to study the dynamics of the system as the critical stability boundary is crossed.

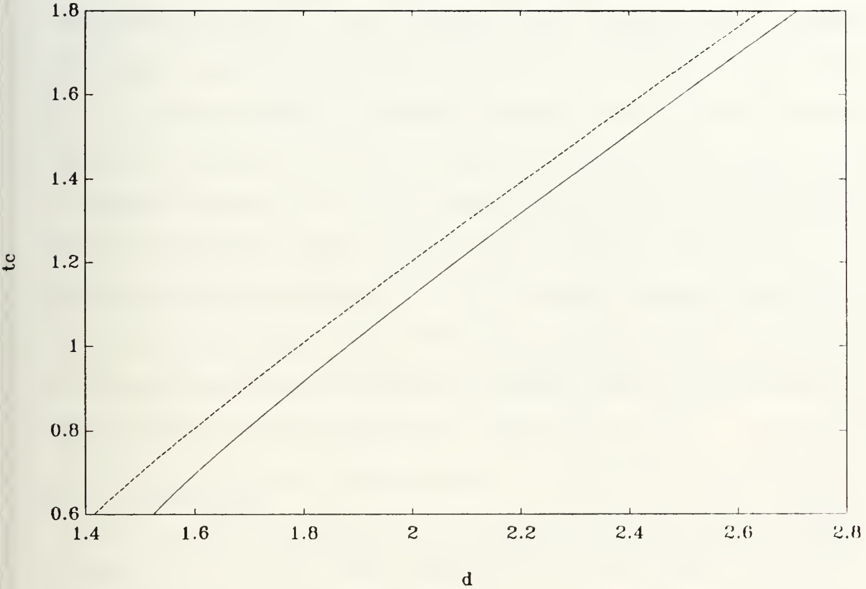

Figure 3. Taylor expansion and Nyquist stability analysis with a one second time lag. (Taylor first order=solid, Taylor second order=dashed, Taylor third order and Nyquist=dotted)

III. HOPF BIFURCATION

A. INTRODUCTION

It can be numerically confirmed that in all cases of stability loss of the previous chapter, one pair of complex conjugate eigenvalues of the corresponding eigenvalue problem crosses transversely the imaginary axis. A situation like this in which a certain parameter is varied such that the real part of one pair of complex conjugate eigenvalues of the linearized system matrix crosses zero, will result in the system leaving its steady state in an oscillatory manner. This loss of stability is called Hopf bifurcation and generically occurs in one of two ways, supercritical or subcritical. In the supercritical case, stable limit cycles are generated after the nominal straight line motion loses its stability. The amplitudes of these limit cycles are continuously increasing as the parameter distance from its critical value is increased. For small values of this criticality distance the resulting limit cycle is of small amplitude and differs little from the initial nominal state. In the subcritical case, however, unstable limit cycles are generated before the nominal state loses its stability. Therefore, depending on the initial conditions it is possible to diverge away from the nominal straight line path and

converge toward a different steady state even before the nominal motion loses its stability. In many cases this new steady state is another limit cycle of considerably higher amplitude. This means that in the subcritical Hopf bifurcation case the domain of attraction of the nominal state is decreasing and in fact it shrinks to zero as the critical point is approached. Random external disturbances of sufficient magnitude can throw the vehicle off to an oscillatory steady state even though the nominal state may still remain stable. After the nominal state becomes unstable, a discontinuous increase in the magnitude of motions is observed as there exists no simple stable nearby attractors for the vehicle to converge to. Distinction between these two qualitatively different types of bifurcation is, therefore, essential in design. The computational procedure requires higher order approximations in the equations of motion and is the subject of the next section.

B. COMPUTATIONS

The vehicle equations of motion are written in the form

$$\psi = r \tag{3.1a}$$

$$\dot{v} = a_{11}uv + a_{12}ur + b_1u^2\delta \tag{3.1b}$$

$$\dot{r} = a_{21}uv + a_{22}ur + b_2u^2\delta \tag{3.1c}$$

$$\dot{y} = u\sin\psi + v\cos\psi \tag{3.1d}$$

In order to capture the effect of rudder saturation we write the rudder angle δ in the form

$$\delta = \delta_{sat} \tanh(\frac{\delta_0}{\delta_{sat}}) \tag{3.2}$$

where δ_{sat} is the saturation limit of δ, typically set at +0.4 radians. Equation (3.2) is used instead of a hard saturation function because of its smoothness, which is important for the computation in this section. δ_0 is the linear control law of the form

$$\delta_0 = k_1(\psi - \psi_c) + k_2v + k_3r \tag{3.3}$$

where

$$\tan\psi_c = -\frac{y(t-T)}{d} = -\frac{y - T\dot{y}}{d} \tag{3.4}$$

using the first order approximation for y(t-T).

The state equations (3.1) through (3.4) are written in the compact form

$$\dot{x}=f(x) \tag{3.5}$$

where f(x) is a nonlinear function of the state variables vector

$$x=[\psi, v, r, y] \tag{3.6}$$

Expanding f(x) in Taylor series, we can write (3.5) in the form

$$\dot{x}=Ax+g(x) \tag{3.7}$$

where **A** is the linear system matrix and g(x) contains all the leading nonlinear terms of f(x). Due to the port/starboard symmetry of our problem, g(x) contains only third order terms. Defining **T** as the matrix of eigenvalues of **A** and applying the transformation

$$x=Tz \tag{3.8}$$

the state equation is transformed into its canonical form

$$\dot{z}=T^{-1}ATz+T^{-1}g(Tz) \tag{3.9}$$

At the Hopf bifurcation point

$$T^{-1}AT=\begin{vmatrix}0 & -\omega_0 & 0 & 0\\ \omega_0 & 0 & 0 & 0\\ 0 & 0 & p & 0\\ 0 & 0 & 0 & q\end{vmatrix} \tag{3.10}$$

where p and q are negative and ω_0 is positive. In the new system of coordinates

$$z=T^{-1}x \tag{3.11}$$

the dynamics of the system are generated by a reduced two dimensional system z_1 and z_2, since the coordinates z_3 and z_4 correspond to the eigenvalues p and q and are asymptotically stable. These stable variables z_3, z_4 can be expressed as a function of the critical variables z_1, z_2; these functional expressions are at least of third order. Therefore, the stable coordinates z_3, z_4 do not influence the third order expansion of (3.7). Using the above expression, we can write the two dimensional system in z_1, z_2 as

$$\dot{z}_1=-\omega_0 z_2+r_{11}z_1^3+r_{12}z_1^2z_2+r_{13}z_1z_2^2+r_{14}z_2^3 \tag{3.12a}$$

$$\dot{z}_2=\omega_0 z_1+r_{21}z_1^3+r_{22}z_1^2z_2+r_{23}z_1z_2^2+r_{24}z_2^3 \tag{3.12b}$$

where the coefficients r_{ij} are complicated expressions that are derived from (3.9)

Equations (3.12) are valid at exactly the Hopf bifurcation point. For values of the parameter d close to the bifurcation point, they are written as

$$\dot{z}_1 = \alpha'\varepsilon z_1 - (\omega_0 + \omega'\varepsilon) z_2 + F_1(z_1, z_2) \tag{3.13a}$$

$$\dot{z}_2 = (\omega_0 + \omega'\varepsilon) z_1 + \alpha'\varepsilon z_2 + F_2(z_1, z_2) \tag{3.13b}$$

where α', ω' are the derivatives of the real and imaginary parts of the critical pair of eigenvalues evaluated at the bifurcation point; ε is the difference of the parameter d from its critical value; and the nonlinear function F_1, F_2 remain the same as in (3.12),

$$F_1(z_1, z_2) = r_{11} z_1^3 + r_{12} z_1^2 z_2 + r_{13} z_1 z_2^2 + r_{14} z_2^3 \tag{3.14a}$$

$$F_2(z_1, z_2) = r_{21} z_1^3 + r_{22} z_1^2 z_2 + r_{23} z_1 z_2^2 + r_{24} z_2^3 \tag{3.14b}$$

If we introduce polar coordinates in the form

$$z_1 = R\cos\theta \tag{3.15a}$$

$$z_2 = R\sin\theta \tag{3.15b}$$

equations (3.13) become

$$\dot{R}=\alpha'\varepsilon R+F_1(R,\theta)\cos\theta+F_2(R,\theta)\sin\theta \tag{3.16a}$$

$$R\dot{\theta}=(\omega_0+\omega'\varepsilon)R+F_2(R,\theta)\cos\theta-F_1(R,\theta)\sin\theta \tag{3.16b}$$

Equation (3.16a) yields

$$\dot{R}=\alpha'\varepsilon R+P(\theta)R^3 \tag{3.17}$$

where $P(\theta+2\pi)=P(\theta)$. If (3.17) is averaged over one cycle in θ, we get an equation with constant coefficients

$$\dot{R}=\alpha'\varepsilon R+KR^3 \tag{3.18}$$

where

$$K=\frac{1}{2\pi}\int_0^{2\pi}P(\theta)\,d\theta \tag{3.19}$$

Carrying out the indicated integration in (3.19) we obtain

$$K=\frac{1}{8}(3r_{11}+r_{13}+r_{22}+3r_{24}) \tag{3.20}$$

Existence and stability of limit cycles can be determined by analyzing the equilibrium points of the averaged equation (3.18), which correspond to periodic solutions in z_1, z_2 as can be seen from (3.15). If we examine equation (3.18) we can see that:

1) If $\alpha'>0$, then:

(a) If $K>0$ then unstable limit cycles coexist with the stable equilibrium for $\varepsilon<0$.

(b) If $K<0$ then stable limit cycles coexist with the unstable equilibrium for $\varepsilon>0$.

2) If $\alpha'<0$, then:

(a) If $K>0$ then unstable limit cycles coexist with the stable equilibrium for $\varepsilon>0$.

(b) If $K<0$ then stable limit cycles coexist with the unstable equilibrium for $\varepsilon<0$.

Therefore, we can see that computation of the above nonlinear coefficient K can distinguish between the two different types of Hopf bifurcation:

- Supercritical if $K<0$
- Subcritical if $K>0$

[Ref. 10].

C. RESULTS

Values of the coefficient K have been calculated for several different values of a y position information time lag, over a span of system time constants, using the Fortran program presented in appendix A. This program has also been used to determine the vehicle period of oscillation in the same conditions. Figure 4 shows the behavior of the K coefficient at three different time lags, and Figure 5 shows periods of oscillation at the same three time lags. It can be

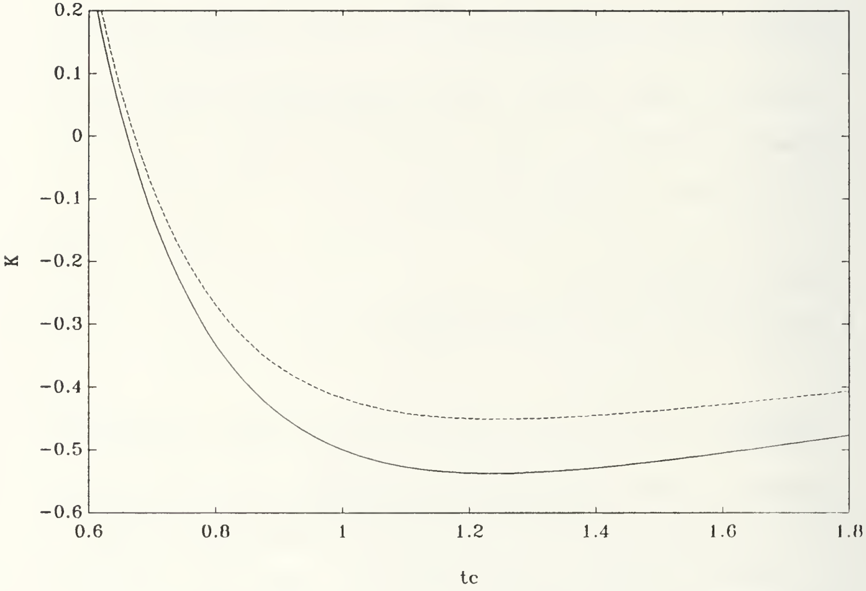

Figure 4. Coefficient K versus t_c at three values of time lag T. (0.5 sec=solid, 1.0 sec=dashed, 1.5 sec=dotted)

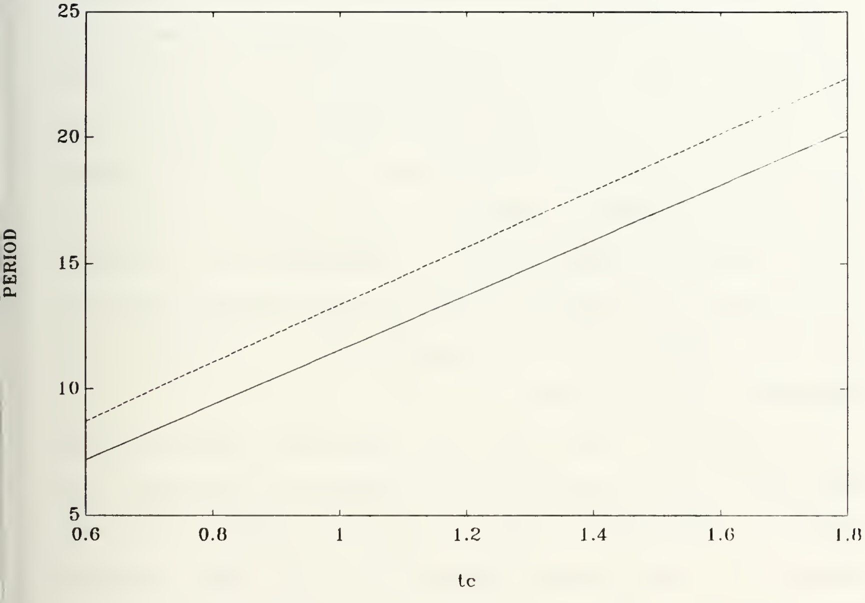

Figure 5. Vehicle oscillation period versus t_c for three values of time lag T. (0.5 sec=solid, 1.0 sec=dashed, 1.5 sec=dotted)

seen that supercritical bifurcations are ensured for sufficiently high values of the control time constant t_c. For t_c less than a certain critical value, the corresponding Hopf bifurcations are subcritical. This situation should be avoided in practice.

D. SIMULATIONS

The vehicle path has been simulated by using the Euler integration method coded in a Fortran program presented in appendix B. The vehicle control law (2.17) as well as the control gains (2.13) are used. The program has been run with input values for system time constant, y position information time lag, and lookahead distance. The vehicle was given an initial nominal y offset of half a shiplength and a nominal forward speed. The resulting plots of y position against time show the vehicle's oscillatory path either converge to the commanded path or diverge.

The results of these simulation runs were compared to the results of the Hopf bifurcation computations in two ways. The period of oscillation observed in the vehicle path was compared to the period predicted by the Hopf program. Additionally, the vehicle stability, determined by convergence to the commanded path, was compared to the K coefficient sign prediction of stability which was determined by the Hopf computations. Figure 6 shows a vehicle path in stable conditions. Figure 7 shows a vehicle path in unstable

conditions. These simulations were chosen in the supercritical bifurcation case and it can be seen that the period of oscillation observed from Figures 7 agrees very well with the theoretical results of Figure 5.

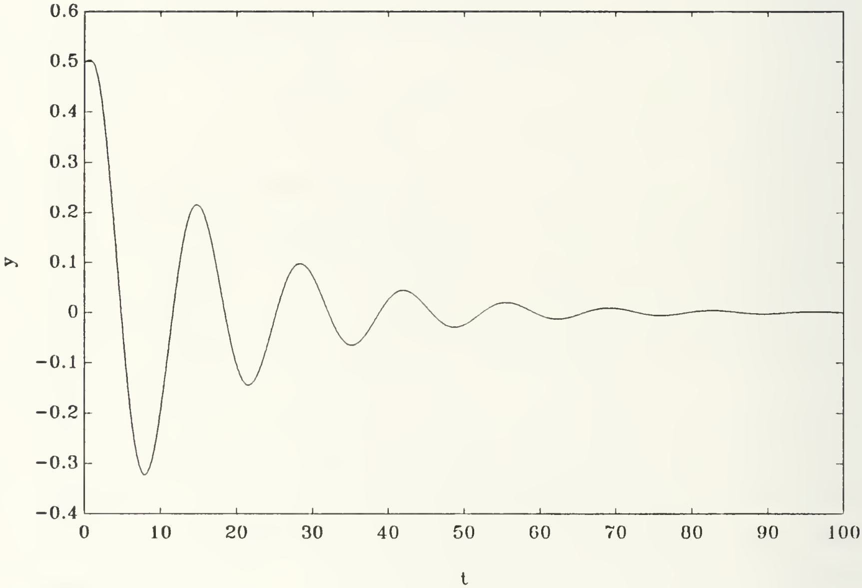

Figure 6. Vehicle path in stable conditions where time constant t_c = 1.0 sec, time lag T = 1.0 sec, and lookahead distance d = 2 shiplengths.

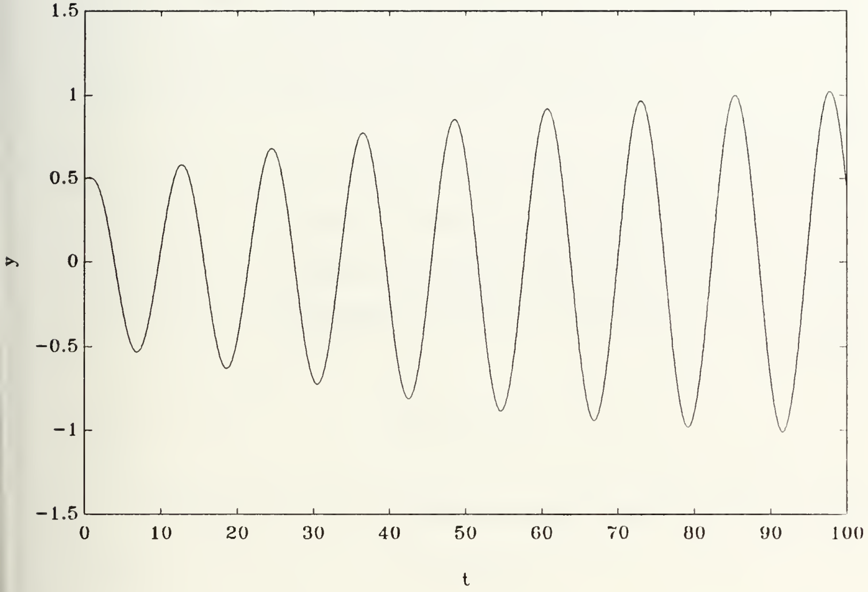

Figure 7. **Vehicle path in unstable conditions where time constant t_c = 1.0 sec, time lag T = 1.0 sec, and lookahead distance d = 1.25 shiplength.**

IV. STABILITY ENHANCEMENT

A. TWO-POINT FORMULA

The time lag of y position information discussed in chapter II has thus far been represented by a single piece of information used in the control law with some delay assigned to it. In an attempt to improve stability with regard to this delay, the use of the previous two positions in the control was examined.

Equation (2.15) shows the representation of the time delay, and equation (2.16) shows its effect on the control law. A straight line approximation is applied to the previous two positions as shown in Figure 8. The general y position is defined by

$$y(t)=a_1t+a_2 \tag{4.1}$$

The two previous positions become

$$y_1=a_1t_1+a_2 \tag{4.2a}$$

$$y_2=a_1t_2+a_2 \tag{4.2b}$$

The coefficients a_1 and a_2 are stated as

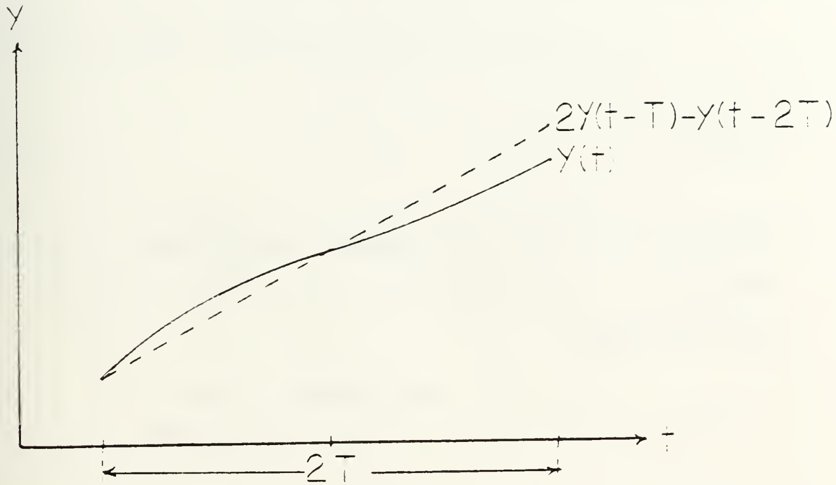

Figure 8. Straight line approximation using two previous positions.

$$a_1 = \frac{y_1 - y_2}{t_1 - t_2} \quad (4.3a)$$

$$a_2 = \frac{y_1 t_2 - y_2 t_1}{t_2 - t_1} \quad (4.3b)$$

The previous time values are represented as

$$t_1 = t - 2T \quad (4.4a)$$

$$t_2 = t - T \quad (4.4b)$$

where T is the time lag associated with the y position information. The previous positions, in terms of the previous time values are

$$y_1 = y(t - 2T) \quad (4.5a)$$

$$y_2 = y(t - T) \quad (4.5b)$$

Substitution and algebra gives a general position expression of

$$y(t) = 2y(t - T) - y(t - 2T) \quad (4.6)$$

B. STABILITY ANALYSIS

The Laplace transform of equation (4.6) is

$$y(t) = y(2e^{-Ts} - e^{-2Ts}) \tag{4.7}$$

The control law becomes

$$\delta = k_1\psi + k_2 v + k_3 r + \frac{k_1}{d} y(2e^{-Ts} - e^{-2Ts}) \tag{4.8}$$

and the linearized equations of motion become

$$\psi = r \tag{4.9a}$$

$$\begin{aligned}\dot{v} = {} & b_1 u^2 k_1 \psi + (a_{11}u + b_1 u^2 k_2)\, v + (a_{12}u + b_1 u^2 k_3)\, r \\ & + b_1 u^2 \frac{k_1}{d} y(2e^{-Ts} - e^{-2Ts})\end{aligned} \tag{4.9b}$$

$$\begin{aligned}\dot{r} = {} & b_2 u^2 k_1 \psi + (a_{12}u + b_2 u^2 k_2)\, v + (a_{22}u + b_2 u^2 k_3)\, r \\ & + b_2 u^2 \frac{k_1}{d} y(2e^{-Ts} - e^{-2Ts})\end{aligned} \tag{4.9c}$$

$$\dot{y} = u\psi + v \tag{4.9d}$$

These motion equations reduce to the state space form

$$\dot{x} = Ax \tag{4.10}$$

The matrix form becomes

$$\begin{vmatrix} \dot{\psi} \\ \dot{v} \\ \dot{r} \\ \dot{y} \end{vmatrix} = \begin{vmatrix} 0 & 0 & 1 & 0 \\ b_1 u^2 k_1 & a_{11}u+b_1 u^2 k_2 & a_{12}u+b_1 u^2 k_3 & b_1 u^2 \frac{k_1}{d}(2e^{-Ts}-e^{-2Ts}) \\ b_2 u^2 k_1 & a_{21}u+b_2 u^2 k_2 & a_{22}u+b_2 u^2 k_3 & b_2 u_2 \frac{k_1}{d}(2e^{-Ts}-e^{-2Ts}) \\ u & 1 & 0 & 0 \end{vmatrix} \begin{vmatrix} \psi \\ v \\ r \\ y \end{vmatrix}$$

The characteristic equation of the form [A-Is]=0 is

$$s^4+A_3 s^3+A_2 s^2+A_1 s+(B_2 s^2+b_1 s+B_0)D(2e^{-Ts}-e^{-2Ts}) \qquad (4.11)$$

where

$$A_3=-(a_{11}+a_{22})u-(b_1 k_2+b_2 k_3)u^2$$

$$A_2=(a_{11}a_{22}-a_{12}a_{21})u^2+(a_{11}b_2-a_{21}b_1)u^3 k_3+(a_{22}b_1-a_{12}b_2)u^3 k_2-b_2 u^2 k_1$$

$$A_1=-(a_{21}b_1-a_{11}b_2)u^3 k_1$$

$$B_2=-b_1 u^2 k_1$$

$$B_1=-b_2 u^3 k_1-(a_{12}b_2-a_{22}b_1)u^3 k_1$$

$$B_0 = (a_{11}b_2 - a_{21}b_1)\, u^4 k_1$$

$$D = \frac{1}{d}$$

The characteristic equation of the system is written as

$$1 + KG(s) = 0 \tag{4.12}$$

where

$$G(s) = \frac{(B_2 s^2 + B_1 s + B_0)\,(2e^{-Ts} - e^{-2Ts})}{s\,(s^3 + A_3 s^2 + A_2 s + A_1)} \tag{4.13}$$

is the transfer function, and we have denoted

$$K = D \tag{4.14}$$

With s=jω, the phase angle is represented by

$$\phi = \angle G(j\omega) \tag{4.15}$$

where

$$\begin{aligned}\phi = &\angle(2e^{-Tj\omega} - e^{-2Tj\omega}) - \angle(j\omega) + \angle(-B_2\omega^2 + B_1 j\omega + B_0) \\ &- \angle(-j\omega^3 - A_3\omega^2 + A_2 j\omega + A_1)\end{aligned}$$

$$\phi = \tan^{-1}\frac{-2\sin(\omega T)+\sin(2\omega T)}{2\cos(\omega T)-\cos(2\omega T)} - \frac{\pi}{2} + \tan^{-1}\left(\frac{B_1\omega}{B_0 - B_2\omega^2}\right) - \tan^{-1}\left(\frac{-\omega^3 - A_2\omega}{-A_3\omega^2 + A_1}\right) \tag{4.16}$$

The Nyquist stability criterion states that at the solution of

$$\phi(\omega) = -\pi \tag{4.17}$$

where ω is the phase cross over frequency ω_1, the gain margin must equal 1

$$|KG(j\omega_1)| = 1 \tag{4.18}$$

where K = D = 1/d. Equation (4.17) becomes

$$\tan^{-1}\frac{-2\sin(\omega_1 T)+\sin(2\omega_1 T)}{2\cos(\omega_1 T)-\cos(2\omega_1 T)} - \frac{\pi}{2} + \tan^{-1}\left(\frac{B_1\omega_1}{B_0 - B_2\omega_1^2}\right) - \tan^{-1}\left(\frac{-\omega_1^3 + A_2\omega_1}{-A_3\omega_1^2 + A_1}\right) = -\pi \tag{4.19}$$

Rearranged as

$$\tan^{-1}\left(\frac{B_1\omega_1}{B_0 - B_2\omega_1^2}\right) - \tan^{-1}\left(\frac{-\omega_1^3 + A_2\omega_1}{-A_3\omega_1^2 + A_1}\right) = -\frac{\pi}{2} - \tan^{-1}\frac{-2\sin(\omega_1 T)+\sin(2\omega_1 T)}{2\cos(\omega_1 T)-\cos(2\omega_1 T)}$$

Taking the tangent of both sides and using the identity

$$\tan(x-y) = \frac{\tan(x)-\tan(y)}{1+\tan(x)\tan(y)}$$

then algebra and rearranging gives

$$\frac{B_1\omega_1(A_1-A_3\omega_1^2)-(B_0-B_2\omega_1^2)(-\omega_1^3+A_2\omega_1)}{(B_0-B_2\omega_1^2)(-A_3\omega_1^2+A_1)+B_1\omega_1(-\omega_1^3+A_2\omega_1)} = \frac{2\cos(\omega_1 T-\cos(2\omega_1 T)}{-2\sin(\omega_1 T)+\sin(2\omega_1 T)} \tag{4.20}$$

The stability computations require an initial value for ω_1. This is accomplished by setting the time lag T=0, and using

$$(B_0-B_2\omega_1^2)(-A_3\omega_1^2+A_1)+B_1\omega_1(-\omega_1^3+A_2\omega_1)=0 \tag{4.21}$$

rearranged as

$$(B_2A_3-B_1)\omega_1^4+(B_1A_2-B_2A_1-B_0A_3)\omega_1^2+B_0A_1=0 \tag{4.22}$$

Setting the gain margin equal to 1 gives

$$\frac{1}{d}\frac{|(-B_2\omega_1^2+B_1j\omega_1+B_0)(2e^{-j\omega_1 T}-e^{-2j\omega_1 T})|}{\omega_1|-j\omega_1^3-A_3\omega_1^2+A_2j\omega_1+A_1|}=1$$

and d can be solved for by

$$d=\frac{\sqrt{(B_0-B_2\omega_1^2)+B^2\omega_1^2}\;\sqrt{5-4\cos(\omega_1 T}}{\omega_1\sqrt{(A_1-A_3\omega_1^2)^2+(A_2\omega_1-\omega_1^3)^2}} \tag{4.23}$$

In order to facilitate computation, terms are grouped as follows

$$\alpha_1=B_2A_3-B_1$$

$$\alpha_2=B_1A_2-B_2A_1-B_0A_3$$

$$\alpha_3=B_0A_1$$

$$\beta_1=-B_2$$

$$\beta_2=B_0+B_2A_2-B_1A_3$$

$$\beta_3=B_1A_1-B_0A_2$$

Equation (4.20) becomes

$$\frac{\beta_1\omega^5+\beta_2\omega^3+\beta_3\omega}{\alpha_1\omega^4+\alpha_2\omega^2+\alpha_3}=\frac{2\cos(\omega T)-\cos(2\omega T)}{-2\sin(\omega T)+\sin(2\omega T)} \tag{4.24}$$

Put in the form

$$f(\omega)=0 \tag{4.25}$$

equation (4.24) becomes

$$\begin{aligned}&[(\beta_1\omega^5+\beta_2\omega^3+\beta_3\omega)(-2\sin(\omega T)+\sin(2\omega T))]\\&\qquad -[(\alpha_1\omega^4+\alpha_2\omega^2+\alpha_3)(2\cos(\omega T)-\cos(2\omega T))]=0\end{aligned} \tag{4.26}$$

Newton's iteration is used as

$$\omega_k=\omega_{k-1}-\frac{f(\omega_{k-1})}{f'(\omega_{k-1})} \tag{4.27}$$

Where the function of ω is

$$\begin{aligned}f(\omega)=&(\beta_1\omega^5+\beta_2\omega^3+\beta_3\omega)(-2\sin(\omega T))\\&+(\beta_1\omega^5+\beta_2\omega^3+\beta_3\omega)(\sin(2\omega T))\\&-(\alpha_1\omega^4+\alpha_2\omega^2+\alpha_3)(2\cos(\omega T))\\&+(\alpha_1\omega^4+\alpha_2\omega^2+\alpha_3)(\cos(2\omega T))\end{aligned} \tag{4.28}$$

and the derivative function is

$$\begin{aligned}f'(\omega)=&(5\beta_1\omega^4+3\beta_2\omega^2+\beta_3)(-2\sin(\omega T))\\&-(\beta_1\omega^5+\beta_2\omega^3+\beta_1\omega)(2T\cos(\omega T)\\&+(5\beta_1\omega^4+3\beta_2\omega^2+\beta_1)(\sin(2\omega T))\\&+(\beta_1\omega^5+\beta_2\omega^3+\beta_3\omega)(2T\cos(2\omega T))\\&+(4\alpha_1\omega^3+2\alpha_2\omega)(-2\cos(\omega T))\\&+(\alpha_1\omega^4+\alpha_2\omega^2+\alpha_3)(2T\sin(\omega T))\\&+(4\alpha_1\omega^3+2\alpha_2\omega)(\cos(2\omega T))\\&-(\alpha_1\omega^4+\alpha_2\omega^2+\alpha_3)(2T\sin(2\omega T))\end{aligned} \tag{4.29}$$

Appendix C presents the Fortran program used to determine stability characteristics as a function of system time constant and time lag.

C. RESULTS AND DISCUSSION

Values for the minimum lookahead distance required for controller stability have been computed as a function of the system time constant and the y position information time lag using the two-point formula. Figures 9, 10, and 11 show critical lookahead distance plotted against time constant at three values of time lag for both the two-point method as well as the single point (Nyquist) method discussed in chapter II. These figures show an overall decrease in required lookahead distance as a result of the use of the two-point memory model. An exception to this occurs at low values of t_c. However, these values are to be avoided in practice, as explained in the previous chapter.

Figure 12 through 15 show the critical lookahead distance plotted against time lag for different values of the time constant using both the two-point and single point methods. Again the two-point method produces superior results to the single point method, with the exception of small time constants and large time lags. The same information is summarized in Figure 16 through 19, where we show the ratio d_2/d_1 (critical lookahead distance using the two-point method divided by the critical lookahead distance using the single

point method) verses time constant and time lag. It can be seen that the use of the two-point method can result in improvement in the region of stability of over 20%.

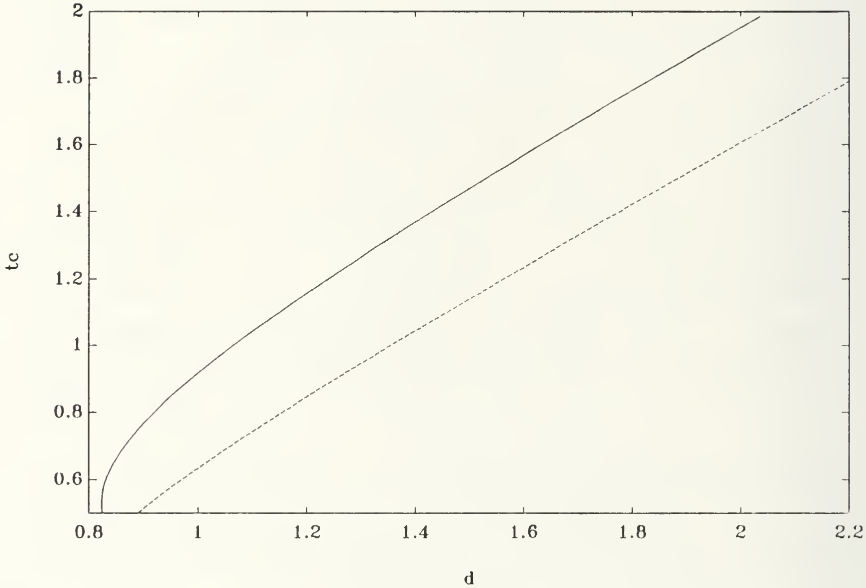

Figure 9. Critical lookahead distance d versus time constant t_c with time lag T = 0.5 sec (two-point method=solid, single point=dashed).

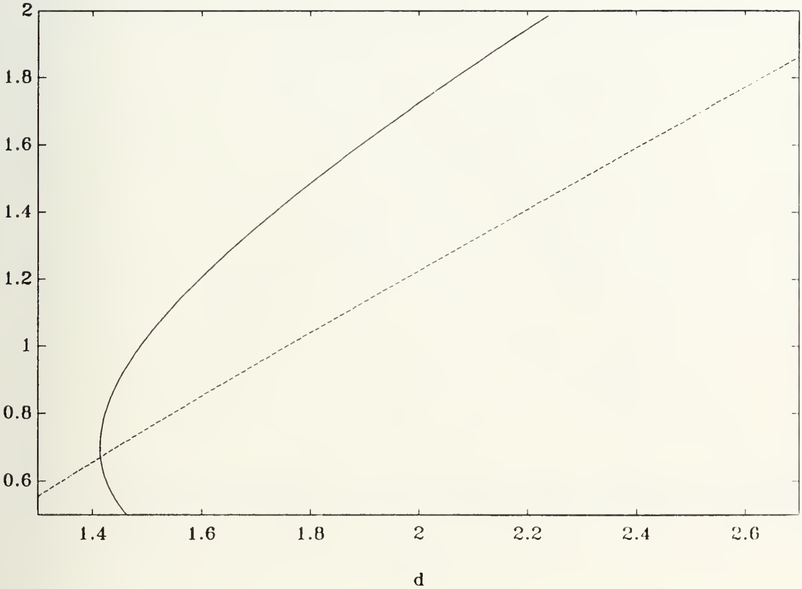

Figure 10. Critical lookahead distance d versus time constant t_c with time lag T = 1.0 sec (two-point method=solid, single point=dashed).

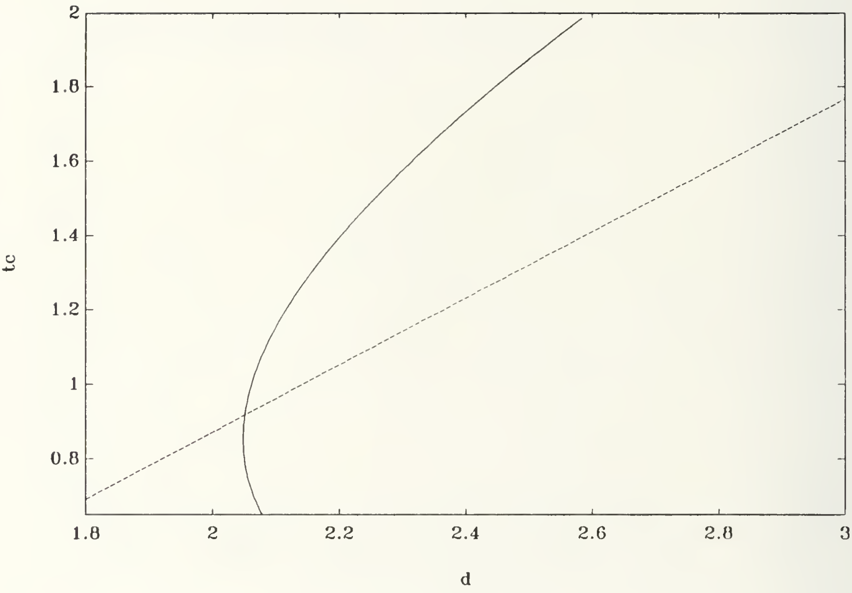

Figure 11. Critical lookahead distance d versus time constant t_c with time lag T = 1.5 sec (two-point method=solid, single point=dashed).

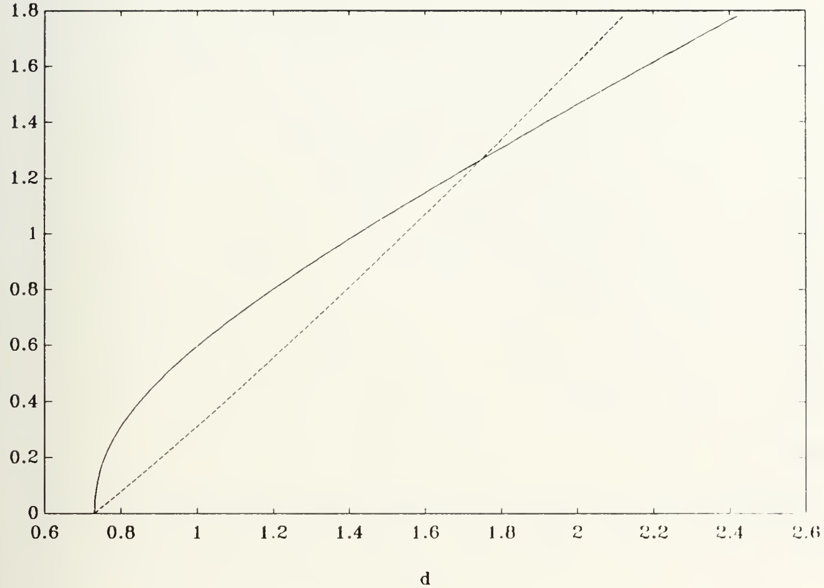

Figure 12. Critical lookahead distance d versus time lag T with time constant t_c = 0.8 sec (two-point method=solid, single point= dashed).

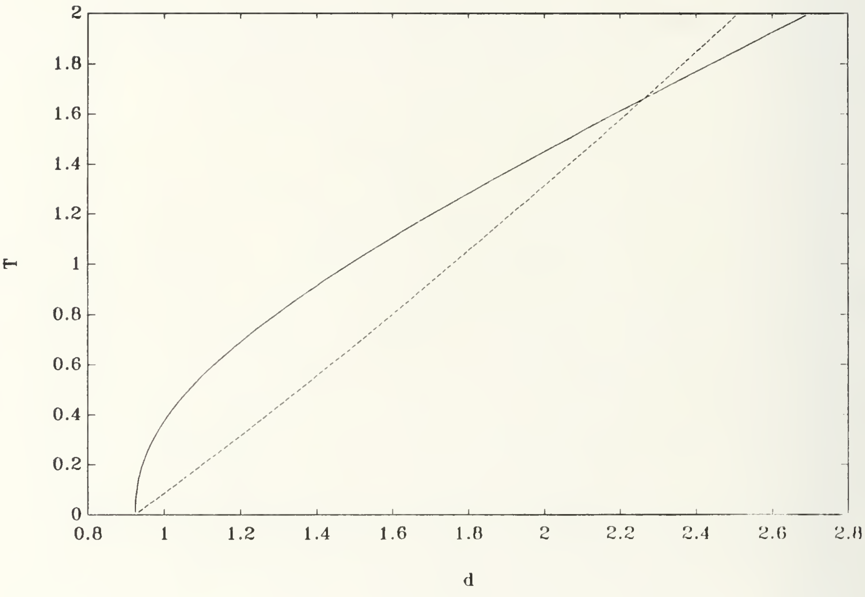

Figure 13. Critical lookahead distance d versus time lag T with time constant t_c = 1.0 sec (two-point method=solid, single point= dashed).

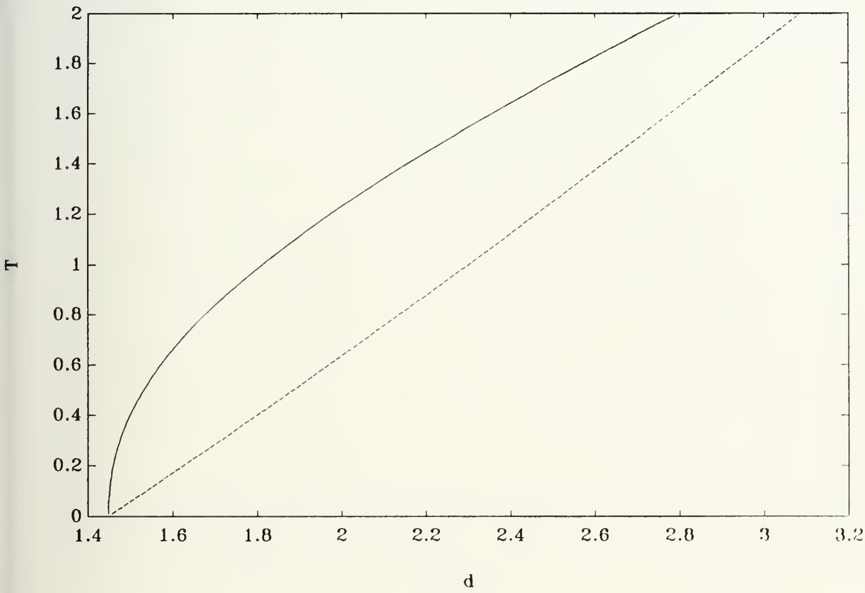

Figure 14. Critical lookahead distance d versus time lag T with time constant t_c = 1.5 sec (two-point method=solid, single point=dashed).

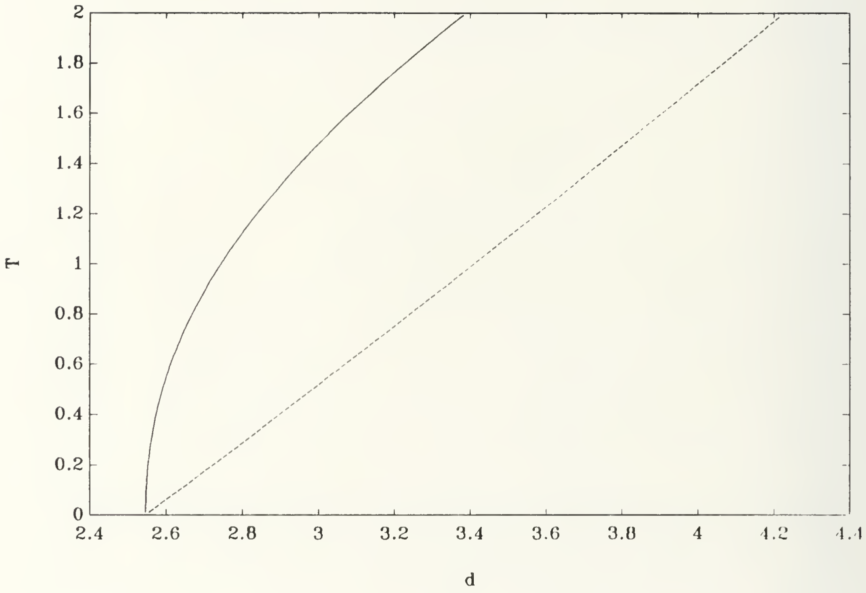

Figure 15. Critical lookahead distance d versus time lag T with time constant t_c = 2.5 sec (two-point method=solid, single point=dashed).

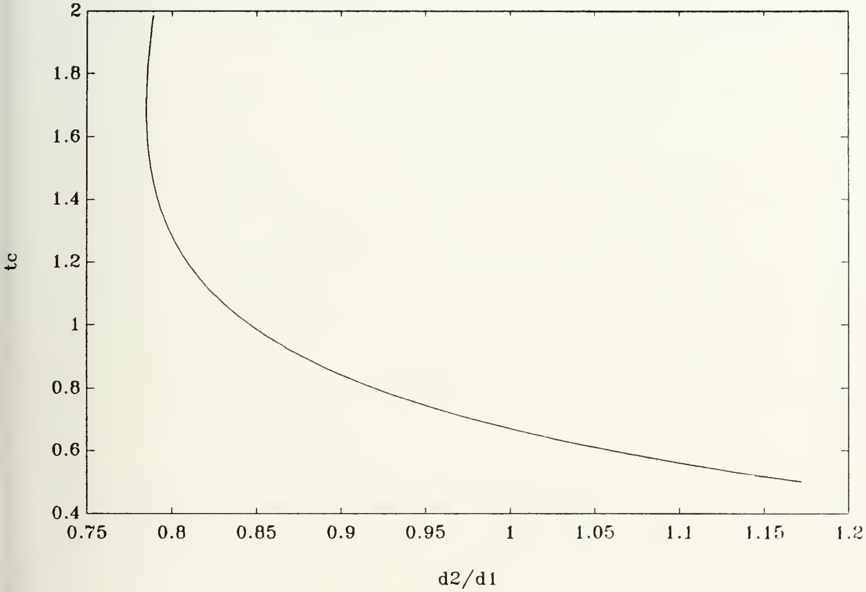

Figure 16. Ratio d_2/d_1 versus time constant t_c with time lag = 1.0 sec.

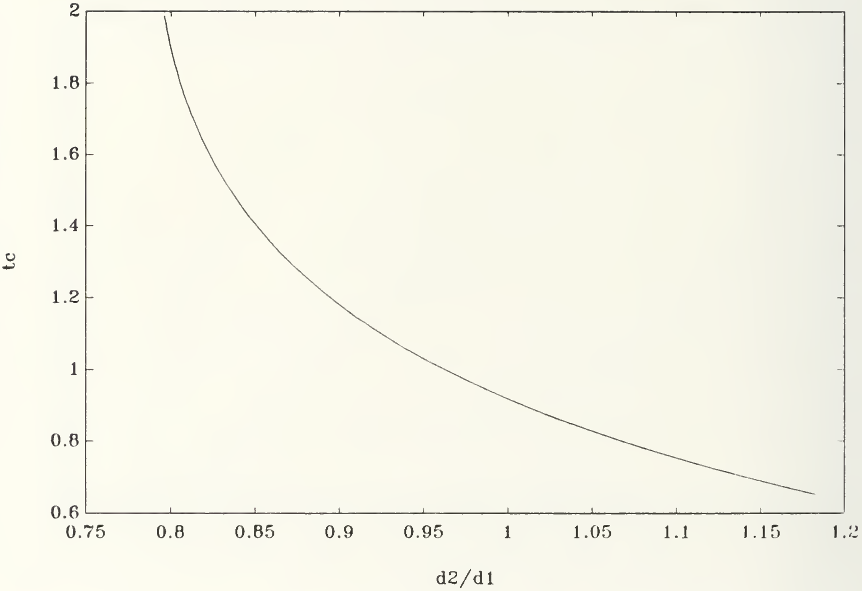

Figure 17. Ratio d_2/d_1 versus time constant t_c with time lag = 1.5 sec.

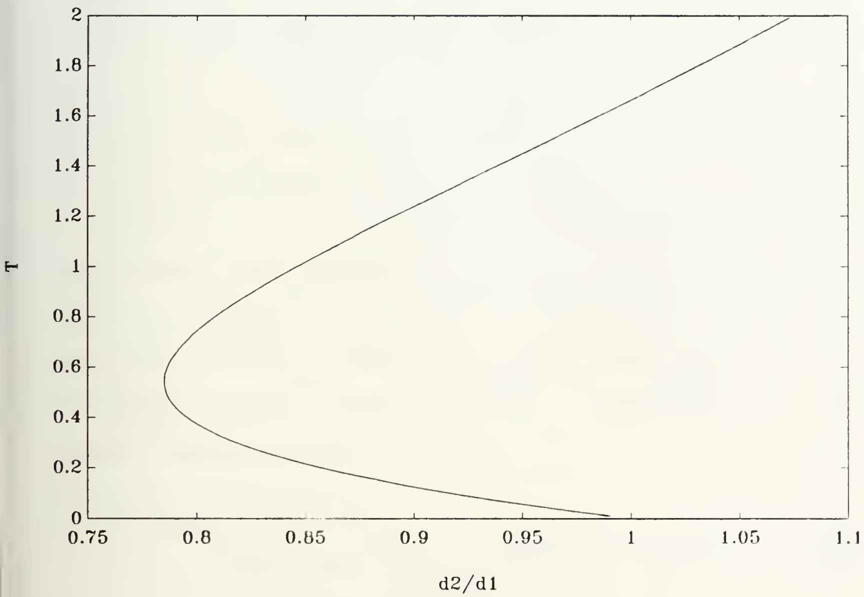

figure 18. Ratio d_2/d_1 versus time lag T with time constant = 1.0 sec

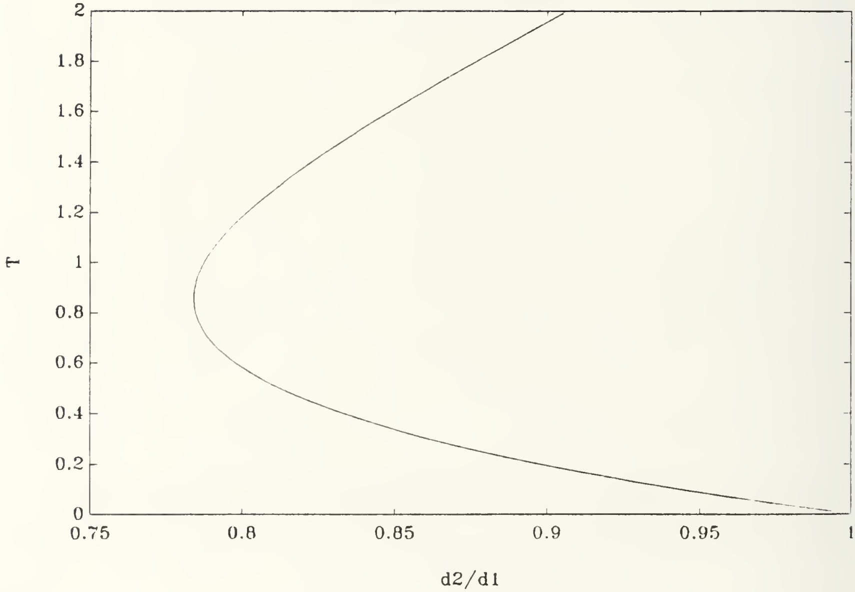

Figure 19. Ratio d_2/d_1 versus time lag T with time constant = 1.5 sec.

V. CONCLUSIONS AND RECOMMENDATIONS

A. CONCLUSIONS

Nonlinear bifurcation theory has been applied to the NPS autonomous underwater vehicle through a Hopf bifurcation analysis of the vehicle's navigation guidance and control scheme. It has been shown that under normal conditions the vehicle will operate in the supercritical region, and therefore the unpredictable behavior associated with the subcritical case should not to be expected.

Secondly, the control scheme was modified by the use of a single stage memory model which incorporates the two previous vehicle positions in the linearized control law. It has been shown that the use of this memory model reduces the vehicle's required lookhead distance for control stability within the normal operating range.

B. RECOMMENDATIONS

In the event that not all of the state information required is directly available through measurements, the control/guidance scheme would include an observer. The effect of the observer dynamics on the higher order nonlinear terms, and therefore on the bifurcation limit cycle stability, should be examined.

APPENDIX A

```
C       PROGRAM HOPF.FOR
C
C       Hopf Bifurcation Analysis
C
C       Critical Point:          Exact
C       Third Order Expansions:  First Order Approximation
C
        IMPLICIT DOUBLE PRECISION (A-H,O-Z)
        DOUBLE PRECISION K1,K2,K3,K4,L,NR,NV,NDRS,NDRB,IZ,MASS,
     &                   NRDOT,NVDOT,K1P,K2P
        DOUBLE PRECISION M11,M12,M13,M14,M21,M22,M23,M24,
     1                   M31,M32,M33,M34,M41,M42,M43,M44,
     2                   N11,N12,N13,N14,N21,N22,N23,N24,
     3                   N31,N32,N33,N34,N41,N42,N43,N44,
     4                   L21,L22,L23,L24,L31,L32,L33,L34,
     5                   L41,L42,L43,L44
C
        DIMENSION A(4,4),T(4,4),TINV(4,4),FV1(4),IV1(4),ZZZ(4,4)
        DIMENSION WR(4),WI(4),TSAVE(4,4),TLUD(4,4),IVLUD(4),SVLUD(4)
        DIMENSION ASAVE(4,4)
C
        OPEN (11,FILE='HOPF.DAT',STATUS='NEW')
        OPEN (12,FILE='PERI.DAT',STATUS='NEW')
        OPEN (13,FILE='ALPH10.DAT',STATUS='NEW')
C
C       Vehicle Parameters
C
        WEIGHT=435.0
        IZ    =45.0
        L     =7.3
        RHO   =1.94
        G     =32.2
        XG    =0.0104
        MASS  =WEIGHT/G
        U     =5.0
        RATIO =0.0
        D0    =0.4
C        WRITE (*,1006)
C        READ  (*,*) D0
C
        YRDOT =-0.00178*0.5*RHO*L**4
        YVDOT =-0.03430*0.5*RHO*L**3
        YR    =+0.01187*0.5*RHO*L**3
        YV    =-0.03896*0.5*RHO*L**2
        YDRS  =+0.02345*0.5*RHO*L**2
        YDRB  =+0.02345*0.5*RHO*L**2
        NRDOT =-0.00047*0.5*RHO*L**5
        NVDOT =-0.00178*0.5*RHO*L**4
        NR    =-0.01022*0.5*RHO*L**4
        NV    =-0.00769*0.5*RHO*L**3
```

```
)RS   =-0.337*0.02345*0.5*RHO*L**3
)RB   =+0.283*0.02345*0.5*RHO*L**3

I  =(IZ-NRDOT)*(MASS-YVDOT)-
    (MASS*XG-YRDOT)*(MASS*XG-NVDOT)
\11=((IZ-NRDOT)*YV-(MASS*XG-YRDOT)*NV)/DH
\12=((IZ-NRDOT)*(-MASS+YR)-
    (MASS*XG-YRDOT)*(-MASS*XG+NR))/DH
\21=((MASS-YVDOT)*NV-(MASS*XG-NVDOT)*YV)/DH
\22=((MASS-YVDOT)*(-MASS*XG+NR)-
    (MASS*XG-NVDOT)*(-MASS+YR))/DH
311=((IZ-NRDOT)*YDRS-(MASS*XG-YRDOT)*NDRS)/DH
312=((IZ-NRDOT)*YDRB-(MASS*XG-YRDOT)*NDRB)/DH
321=((MASS-YVDOT)*NDRS-(MASS*XG-NVDOT)*YDRS)/DH
322=((MASS-YVDOT)*NDRB-(MASS*XG-NVDOT)*YDRB)/DH


31=BB11+RATIO*BB12
32=BB21+RATIO*BB22

RITE (*,1005)
EAD  (*,*)    TL
RITE (*,1001)
EAD  (*,*)    TC


PS=1.D-10
TMAX=1000

TL=0.5
DO 50 M=1,100
.D=TL*L/U

TC=0.5
) 40 K=1,100
 TCD=TC*L/U
 POLEC=1.0/TCD
 AD1=3.0*POLEC
 AD2=3.0*POLEC**2
 AD3=POLEC**3
 A1=BB1*U*U
 B1=BB2*U*U
 C1=-AD1-(AA11+AA22)*U
 A2=(BB1*AA22-BB2*AA12)*U**3
 B2=(BB2*AA11-BB1*AA21)*U**3
 K1=AD3/((BB2*AA11-BB1*AA21)*U**3)
 C2=AD2-(AA11*AA22-AA12*AA21)*U**2+BB2*U*U*K1
 K2=(C1*B2-C2*B1)/(A1*B2-A2*B1)
 K3=(C2*A1-C1*A2)/(A1*B2-A2*B1)

 A1= (AA11*BB2-AA21*BB1)*U*U*U*K1
 A2= (AA11*AA22-AA12*AA21)*U*U+(AA11*BB2-AA21*BB1)*U*U*U*K3+
     (AA22*BB1-AA12*BB2)*U*U*U*K2-BB2*U*U*K1
 A3=-(AA11+AA22)*U-(BB1*K2+BB2*K3)*U*U
 B0= (AA11*BB2-AA21*BB1)*U*U*U*U*K1
 B1=-(AA12*BB2-AA22*BB1)*U*U*U*K1-BB2*U*U*U*K1
 B2=-BB1*U*U*K1

 Compute Initial Approximation For Omega (TL=0)
```

```
      AQ=B2*A3-B1
      BQ=B1*A2-B2*A1-B0*A3
      CQ=B0*A1
      DET=BQ**2-4.D0*AQ*CQ
      IF (DET.LT.0.D0) GO TO 40
      ZT1=(-BQ+DSQRT(DET))/(2.0D0*AQ)
      ZT2=(-BQ-DSQRT(DET))/(2.0D0*AQ)
      IF (ZT1.GE.0.D0) OM=DSQRT(ZT1)
      IF (ZT2.GE.0.D0) OM=DSQRT(ZT2)
      ALPHA1=AQ
      ALPHA2=BQ
      ALPHA3=CQ
      BETA1=-B2
      BETA2=B0+B2*A2-B1*A3
      BETA3=B1*A1-B0*A2
C
C     Compute Exact Omega Using Newton's Iteration
C
      OMOLD=OM
 93   F=(BETA1*OMOLD**5+BETA2*OMOLD**3+BETA3*OMOLD)*DSIN(OMOLD*TLD)
     &  +(ALPHA1*OMOLD**4+ALPHA2*OMOLD**2+ALPHA3)*DCOS(OMOLD*TLD)
      FPRIME=(5.D0*BETA1*OMOLD**4+3.D0*BETA2*OMOLD**2+BETA3)
     &  *DSIN(OMOLD*TLD)+(BETA1*OMOLD**5+BETA2*OMOLD**3+BETA3*OMOLD)
     &  *TLD*DCOS(OMOLD*TLD)+(4.D0*ALPHA1*OMOLD**3+2.D0*ALPHA2*OMOLD)
     &  *DCOS(OMOLD*TLD)-(ALPHA1*OMOLD**4+ALPHA2*OMOLD**2+ALPHA3)
     &  *TLD*DSIN(OMOLD*TLD)
      IF (FPRIME.EQ.0.D0) STOP 1112
      IF (F.EQ.0.D0) GO TO 92
      OMNEW=OMOLD-F/FPRIME
      OMDIF=DABS(OMNEW-OMOLD)
      IF (OMDIF.LE.EPS) GO TO 92
      OMOLD=OMNEW
      IT=IT+1
      IF (IT.GT.ITMAX) STOP 1111
      GO TO 93
C
 92   OM=OMNEW
      XDNUM=DSQRT((B0-B2*OM**2)**2+(B1*OM)**2)
      XDDEN=OM*DSQRT((A1-A3*OM**2)**2+(A2*OM-OM**3)**2)
      XD=XDNUM/XDDEN
C
C     Start Hopf Bifurcation Analysis
C
C     Evaluate Nonlinear Rudder Expansion Coefficients
C
      K1P=K1-K1*TLD*U/XD
      K2P=K2-K1*TLD/XD
C
      DPPV=- (1.D0/(3.D0*D0**2))*3.D0*K1P*K1P*K2P
     &       + 0.5D0*K1*TLD/XD + 3.D0*K1*(TLD*U)**3/(3.D0*XD**3)
      DPVV=- (1.D0/(3.D0*D0**2))*3.D0*K1P*K2P*K2P
     &       + 3.D0*U*TLD*TLD*TLD*K1/(3.D0*XD**3)
      DPPR=- (1.D0/(3.D0*D0**2))*3.D0*K1P*K1P*K3
      DPRR=- (1.D0/(3.D0*D0**2))*3.D0*K1P*K3*K3
      DPPY=- (1.D0/(3.D0*D0**2))*3.D0*K1P*K1P*K1/XD
     &       - 3.D0*TLD*TLD*U*U*K1/(3.D0*XD**3)
      DPYY=- (1.D0/(3.D0*D0**2))*3.D0*K1P*K1*K1/(XD**2)
     &       + 3.D0*TLD*U*K1/(3.D0*XD**3)
      DVVR=- (1.D0/(3.D0*D0**2))*3.D0*K2P*K2P*K3
      DVRR=- (1.D0/(3.D0*D0**2))*3.D0*K2P*K3*K3
```

```
DVVY=- (1.D0/(3.D0*D0**2))*3.D0*K1*K2P*K2P/XD
     - 3.D0*K1*TLD*TLD/(3.D0*XD**3)
DVYY=- (1.D0/(3.D0*D0**2))*3.D0*K1*K1*K2P/(XD**2)
     + 3.D0*TLD*K1/(3.D0*XD**3)
DRRY=- (1.D0/(3.D0*D0**2))*3.D0*K1*K3*K3/XD
DRYY=- (1.D0/(3.D0*D0**2))*3.D0*K1*K1*K3/(XD**2)
DPVR=- (1.D0/(3.D0*D0**2))*6.D0*K1P*K2P*K3
DPVY=- (1.D0/(3.D0*D0**2))*6.D0*K1P*K1*K2P/XD
     - 6.D0*TLD*TLD*U*K1/(3.D0*XD**3)
DPRY=- (1.D0/(3.D0*D0**2))*6.D0*K1P*K1*K3/XD
DVRY=- (1.D0/(3.D0*D0**2))*6.D0*K1*K2P*K3/XD
DPPP=- (1.D0/(3.D0*D0**2))*1.D0*K1P*K1P*K1P
     + K1*TLD*U/(6.D0*XD) + (K1*(TLD*U)**3)/(3.D0*XD**3)
DVVV=- (1.D0/(3.D0*D0**2))*1.D0*K2P*K2P*K2P
     + K1*(TLD**3)/(3.D0*XD**3)
DRRR=- (1.D0/(3.D0*D0**2))*1.D0*K3*K3*K3
DYYY=- (1.D0/(3.D0*D0**2))*(K1/XD)**3-K1/(3.D0*XD**3)
     - K1/(3.D0*XD**3)

Evaluate Transformation Matrix of Eigenvectors

PSI =0.D0
Y   =0.D0
V   =0.D0
DPSI=K1P
DV  =K2P
DR  =K3
DY  =K1*XD/(XD**2+Y**2)
A(1,1)=0.0D0
A(1,2)=0.0D0
A(1,3)=1.0D0
A(1,4)=0.0D0
A(2,1)=         BB1*U*U*DPSI
A(2,2)=AA11*U+BB1*U*U*DV
A(2,3)=AA12*U+BB1*U*U*DR
A(2,4)=         BB1*U*U*DY
A(3,1)=         BB2*U*U*DPSI
A(3,2)=AA21*U+BB2*U*U*DV
A(3,3)=AA22*U+BB2*U*U*DR
A(3,4)=         BB2*U*U*DY
A(4,1)=U*DCOS(PSI)-V*DSIN(PSI)
A(4,2)=  DCOS(PSI)
A(4,3)=0.0D0
A(4,4)=0.0D0
DO 11 I=1,4
  DO 12 J=1,4
    ASAVE(I,J)=A(I,J)
  CONTINUE
CONTINUE
CALL RG(4,4,A,WR,WI,1,ZZZ,IV1,FV1,IERR)
CALL DSOMEG(IEV,WR,WI,OMEGA,CHECK)
OMEGA0=OMEGA
DO 5 I=1,4
  T(I,1)= ZZZ(I,IEV)
  T(I,2)=-ZZZ(I,IEV+1)
CONTINUE
IF (IEV.EQ.1) GO TO 13
IF (IEV.EQ.2) GO TO 14
IF (IEV.EQ.3) GO TO 15
STOP 3004
```

```
        T(I,3)=ZZZ(I,1)
        T(I,4)=ZZZ(I,4)
  6   CONTINUE
      GO TO 17
 15   DO 7 I=1,4
        T(I,3)=ZZZ(I,1)
        T(I,4)=ZZZ(I,2)
  7   CONTINUE
      GO TO 17
 13   DO 16 I=1,4
        T(I,3)=ZZZ(I,3)
        T(I,4)=ZZZ(I,4)
 16   CONTINUE
 17   CONTINUE
C
C     Normalization of the Critical Eigenvector
C
      CALL NORMAL(T)
C
C     Definition of Mij
C
      M11=T(1,1)
      M21=T(2,1)
      M31=T(3,1)
      M41=T(4,1)
      M12=T(1,2)
      M22=T(2,2)
      M32=T(3,2)
      M42=T(4,2)
      M13=T(1,3)
      M23=T(2,3)
      M33=T(3,3)
      M43=T(4,3)
      M14=T(1,4)
      M24=T(2,4)
      M34=T(3,4)
      M44=T(4,4)
C
C     Definition of Lij
C
      L21= DPPV*M11*M11*M21 + DPVV*M11*M21*M21 + DPPR*M11*M11*M31
     &   + DPRR*M11*M31*M31 + DPPY*M11*M11*M41 + DPYY*M11*M41*M41
     &   + DVVR*M21*M21*M31 + DVRR*M21*M31*M31 + DVVY*M21*M21*M41
     &   + DVYY*M21*M41*M41 + DRRY*M31*M31*M41 + DRYY*M31*M41*M41
     &   + DPVR*M11*M21*M31 + DPVY*M11*M21*M41 + DPRY*M11*M41*M31
     &   + DVRY*M21*M41*M31 + DPPP*M11*M11*M11 + DVVV*M21*M21*M21
     &   + DRRR*M31*M31*M31 + DYYY*M41*M41*M41
C
      PPV = M11*M11*M22 + 2.0*M11*M12*M21
      PVV = M12*M21*M21 + 2.0*M11*M21*M22
      PPR = M11*M11*M32 + 2.0*M11*M12*M31
      PRR = M12*M31*M31 + 2.0*M11*M31*M32
      PPY = M11*M11*M42 + 2.0*M11*M12*M41
      PYY = M41*M41*M12 + 2.0*M11*M41*M42
      VVR = M21*M21*M32 + 2.0*M31*M21*M22
      VRR = M22*M31*M31 + 2.0*M31*M32*M21
      VVY = M21*M21*M42 + 2.0*M41*M21*M22
      VYY = M22*M41*M41 + 2.0*M41*M42*M21
      RRY = M31*M31*M42 + 2.0*M41*M31*M32
```

```
RYY = M32*M41*M41 + 2.0*M41*M42*M31
PVR = M11*M21*M32+M31*(M11*M22+M12*M21)
PVY = M11*M21*M42+M41*(M11*M22+M12*M21)
PRY = M11*M41*M32+M31*(M11*M42+M12*M41)
VRY = M21*M41*M32+M31*(M21*M42+M22*M41)
PPP = 3.0*M11*M11*M12
VVV = 3.0*M21*M21*M22
RRR = 3.0*M31*M31*M32
YYY = 3.0*M41*M41*M42

L22=DPPV*PPV+DPVV*PVV+DPPR*PPR+DPRR*PRR+DPPY*PPY+DPYY*PYY
   +DVVR*VVR+DVRR*VRR+DVVY*VVY+DVYY*VYY+DRRY*RRY+DRYY*RYY
   +DPVR*PVR+DPVY*PVY+DPRY*PRY+DVRY*VRY+DPPP*PPP+DVVV*VVV
   +DRRR*RRR+DYYY*YYY

PPV = M12*M12*M21 + 2.0*M11*M12*M22
PVV = M11*M22*M22 + 2.0*M12*M21*M22
PPR = M12*M12*M31 + 2.0*M11*M12*M32
PRR = M11*M32*M32 + 2.0*M12*M31*M32
PPY = M12*M12*M41 + 2.0*M11*M12*M42
PYY = M11*M42*M42 + 2.0*M12*M41*M42
VVR = M22*M22*M31 + 2.0*M21*M22*M32
VRR = M21*M32*M32 + 2.0*M22*M31*M32
VVY = M22*M22*M41 + 2.0*M21*M22*M42
VYY = M21*M42*M42 + 2.0*M22*M41*M42
RRY = M32*M32*M41 + 2.0*M31*M32*M42
RYY = M31*M42*M42 + 2.0*M32*M41*M42
PVR = M12*M22*M31 + M32*(M11*M22+M12*M21)
PVY = M12*M22*M41 + M42*(M11*M22+M12*M21)
PRY = M12*M42*M31 + M32*(M11*M42+M12*M41)
VRY = M22*M42*M31 + M32*(M21*M42+M22*M41)
PPP = 3.0*M11*M12*M12
VVV = 3.0*M21*M22*M22
RRR = 3.0*M31*M32*M32
YYY = 3.0*M41*M42*M42

L23=DPPV*PPV+DPVV*PVV+DPPR*PPR+DPRR*PRR+DPPY*PPY+DPYY*PYY
   +DVVR*VVR+DVRR*VRR+DVVY*VVY+DVYY*VYY+DRRY*RRY+DRYY*RYY
   +DPVR*PVR+DPVY*PVY+DPRY*PRY+DVRY*VRY+DPPP*PPP+DVVV*VVV
   +DRRR*RRR+DYYY*YYY

L24= DPPV*M12*M12*M22 + DPVV*M12*M22*M22 + DPPR*M12*M12*M32
   + DPRR*M12*M32*M32 + DPPY*M12*M12*M42 + DPYY*M12*M42*M42
   + DVVR*M22*M22*M32 + DVRR*M22*M32*M32 + DVVY*M22*M22*M42
   + DVYY*M22*M42*M42 + DRRY*M32*M32*M42 + DRYY*M32*M42*M42
   + DPVR*M12*M22*M32 + DPVY*M12*M22*M42 + DPRY*M12*M42*M32
   + DVRY*M22*M42*M32 + DPPP*M12*M12*M12 + DVVV*M22*M22*M22
   + DRRR*M32*M32*M32 + DYYY*M42*M42*M42

L31=L21
L32=L22
L33=L23
L34=L24

L21=L21*BB1*U*U
L22=L22*BB1*U*U
L23=L23*BB1*U*U
L24=L24*BB1*U*U
L31=L31*BB2*U*U
L32=L32*BB2*U*U
```

```
      L33=L33*BB2*U*U
      L34=L34*BB2*U*U
      L41=-0.5*M11*M11*(M21+U*M11/3.0)
      L42=-M11*(M12*M21+0.5*M11*M22+0.5*U*M12*M12)
      L43=-M12*(M11*M22+0.5*M12*M21+0.5*U*M11*M12)
      L44=-0.5*M12*M12*(M22+U*M12/3.0)
C
C     Invert Transformation Matrix
C
      DO 2 I=1,4
        DO 3 J=1,4
          TINV(I,J)=0.0
          TSAVE(I,J)=T(I,J)
 3      CONTINUE
 2    CONTINUE
      CALL DLUD(4,4,TSAVE,4,TLUD,IVLUD)
      DO 4 I=1,4
        IF (IVLUD(I).EQ.0) STOP 3003
 4    CONTINUE
      CALL DILU(4,4,TLUD,IVLUD,SVLUD)
      DO 8 I=1,4
        DO 9 J=1,4
          TINV(I,J)=TLUD(I,J)
 9      CONTINUE
 8    CONTINUE
C
C     Check Inv(T)*A*T
C
      IMULT=2
      IF (IMULT.EQ.1) CALL MULT(TINV,ASAVE,T)
      IF (IMULT.EQ.0) STOP
C
C     Definition of Nij
C
      N11=TINV(1,1)
      N21=TINV(2,1)
      N31=TINV(3,1)
      N41=TINV(4,1)
      N12=TINV(1,2)
      N22=TINV(2,2)
      N32=TINV(3,2)
      N42=TINV(4,2)
      N13=TINV(1,3)
      N23=TINV(2,3)
      N33=TINV(3,3)
      N43=TINV(4,3)
      N14=TINV(1,4)
      N24=TINV(2,4)
      N34=TINV(3,4)
      N44=TINV(4,4)
C
      R11=N12*L21+N13*L31+N14*L41
      R12=N12*L22+N13*L32+N14*L42
      R13=N12*L23+N13*L33+N14*L43
      R14=N12*L24+N13*L34+N14*L44
      R21=N22*L21+N23*L31+N24*L41
      R22=N22*L22+N23*L32+N24*L42
      R23=N22*L23+N23*L33+N24*L43
      R24=N22*L24+N23*L34+N24*L44
C
```

```
Evaluate Alpha' and Omega'

DINC=0.001
XDR =XD+DINC
XDL =XD-DINC
XD  =XDR
PSI =0.D0
Y   =0.D0
V   =0.D0
DPSI=K1P
DV  =K2P
DR  =K3
DY  =K1*XD/(XD**2+Y**2)
A(1,1)=0.0D0
A(1,2)=0.0D0
A(1,3)=1.0D0
A(1,4)=0.0D0
A(2,1)=        BB1*U*U*DPSI
A(2,2)=AA11*U+BB1*U*U*DV
A(2,3)=AA12*U+BB1*U*U*DR
A(2,4)=        BB1*U*U*DY
A(3,1)=        BB2*U*U*DPSI
A(3,2)=AA21*U+BB2*U*U*DV
A(3,3)=AA22*U+BB2*U*U*DR
A(3,4)=        BB2*U*U*DY
A(4,1)=U*DCOS(PSI)-V*DSIN(PSI)
A(4,2)=  DCOS(PSI)
A(4,3)=0.0D0
A(4,4)=0.0D0

CALL RG(4,4,A,WR,WI,0,ZZZ,IV1,FV1,IERR)
CALL DSTABL(DEOS,WR,WI,FREQ)
ALPHR=DEOS
OMEGR=FREQ

XD=XDL
PSI =0.D0
Y   =0.D0
V   =0.D0
DPSI=K1P
DV  =K2P
DR  =K3
DY  =K1*XD/(XD**2+Y**2)
A(1,1)=0.0D0
A(1,2)=0.0D0
A(1,3)=1.0D0
A(1,4)=0.0D0
A(2,1)=        BB1*U*U*DPSI
A(2,2)=AA11*U+BB1*U*U*DV
A(2,3)=AA12*U+BB1*U*U*DR
A(2,4)=        BB1*U*U*DY
A(3,1)=        BB2*U*U*DPSI
A(3,2)=AA21*U+BB2*U*U*DV
A(3,3)=AA22*U+BB2*U*U*DR
A(3,4)=        BB2*U*U*DY
A(4,1)=U*DCOS(PSI)-V*DSIN(PSI)
A(4,2)=  DCOS(PSI)
A(4,3)=0.0D0
A(4,4)=0.0D0
```

```
      CALL DSTABL(DEOS,WR,WI,FREQ)
      ALPHL=DEOS
      OMEGL=FREQ
C
      DALPHA=(ALPHR-ALPHL)/(XDR-XDL)
      DOMEGA=(OMEGR-OMEGL)/(XDR-XDL)
C
C     Evaluation of Hopf Bifurcation Coefficients
C
      COEF1=3.0*R11+R13+R22+3.0*R24
      COEF2=3.0*R21+R23-R12-3.0*R14
      AMU2 =-COEF1/(8.0*DALPHA)
      BETA2=0.25*COEF1
      TAU2 =-(COEF2-DOMEGA*COEF1/DALPHA)/(8.0*OMEGA0)
      PERD  =2.0*3.1415927/OMEGA0
      PER   =PERD*U/L
      X=XD/L
      K4=K1/XD
      WRITE (11,*) TC,COEF1
      WRITE (12,*) TC,PER
      WRITE (13,*) TC,DALPHA
    TC=TC+0.015
 40 CONTINUE
C      TL=TL+0.02
C   50 CONTINUE


 1001 FORMAT (' ENTER TIME CONSTANT')
 1005 FORMAT (' ENTER TIME LAG')
 1006 FORMAT (' ENTER D0')
 2002 FORMAT (5E15.5)
      END
C=========================================================================
      SUBROUTINE DSOMEG(IJK,WR,WI,OMEGA,CHECK)
      IMPLICIT DOUBLE PRECISION (A-H,O-Z)
      DIMENSION WR(4),WI(4)
      CHECK=-1.0D+25
      DO 1 I=1,4
        IF (WR(I).LT.CHECK) GO TO 1
        CHECK=WR(I)
        IJ=I
    1 CONTINUE
      OMEGA=DABS(WI(IJ))
      IF (WI(IJ).GT.0.D0) IJK=IJ
      IF (WI(IJ).LT.0.D0) IJK=IJ-1
      RETURN
      END
C=========================================================================
      SUBROUTINE DSTABL(DEOS,WR,WI,OMEGA)
      IMPLICIT DOUBLE PRECISION (A-H,O-Z)
      DIMENSION WR(4),WI(4)
      DEOS=-1.0D+20
      DO 1 I=1,4
        IF (WR(I).LT.DEOS) GO TO 1
        DEOS=WR(I)
        IJ=I
    1 CONTINUE
      OMEGA=WI(IJ)
      OMEGA=DABS(OMEGA)
```

```
ND
=================================================================
UBROUTINE NORMAL(T)
MPLICIT DOUBLE PRECISION (A-H,O-Z)
IMENSION T(4,4),TNOR(4,4)
FAC=T(1,1)**2+T(1,2)**2
F (DABS(CFAC).LE.(1.D-10)) STOP 4001
NOR(1,1)=1.D0
NOR(2,1)=(T(1,1)*T(2,1)+T(2,2)*T(1,2))/CFAC
NOR(3,1)=(T(1,1)*T(3,1)+T(3,2)*T(1,2))/CFAC
NOR(4,1)=(T(1,1)*T(4,1)+T(4,2)*T(1,2))/CFAC
NOR(1,2)=0.D0
NOR(2,2)=(T(2,2)*T(1,1)-T(2,1)*T(1,2))/CFAC
NOR(3,2)=(T(3,2)*T(1,1)-T(3,1)*T(1,2))/CFAC
NOR(4,2)=(T(4,2)*T(1,1)-T(4,1)*T(1,2))/CFAC
O 1 I=1,4
 DO 2 J=1,2
   T(I,J)=TNOR(I,J)
 CONTINUE
ONTINUE
ETURN
ND
=================================================================
UBROUTINE MULT(TINV,A,T)
MPLICIT DOUBLE PRECISION (A-H,O-Z)
IMENSION TINV(4,4),A(4,4),T(4,4),A1(4,4),A2(4,4)
O 1 I=1,4
 DO 2 J=1,4
   A1(I,J)=0.D0
   A2(I,J)=0.D0
 CONTINUE
ONTINUE
O 3 I=1,4
 DO 4 J=1,4
   DO 5 K=1,4
     A1(I,J)=A(I,K)*T(K,J)+A1(I,J)
   CONTINUE
 CONTINUE
ONTINUE
O 6 I=1,4
 DO 7 J=1,4
   DO 8 K=1,4
     A2(I,J)=TINV(I,K)*A1(K,J)+A2(I,J)
   CONTINUE
 CONTINUE
ONTINUE
O 11 I=1,4
  WRITE (*,101) (A(I,J),J=1,4)
ONTINUE
O 12 I=1,4
  WRITE (*,101) (T(I,J),J=1,4)
ONTINUE
O 10 I=1,4
 WRITE (*,101) (A2(I,J),J=1,4)
ONTINUE
WRITE (*,101) A2(1,1)
RETURN
ORMAT (4E15.5)
ND
```

APPENDIX B

```
   PROGRAM SIMU.FOR (VEHICLE PATH SIMULATION)
 REAL K1,K2,K3,L,NR,NV,NDRS,NDRB,IZ,MASS,
&     NRDOT,NVDOT,K1P,K2P

  OPEN (20,FILE='SIM1.DAT',STATUS='NEW')
   OPEN (30,FILE='SIM2.DAT',STATUS='NEW')

 WEIGHT=435.0
 IZ     =45.0
 L      =7.3
 RHO    =1.94
 G      =32.2
 XG     =0.0104
 MASS   =WEIGHT/G
 U      =5.0
 RATIO  =0.0
 D0     =0.4
 XG     =XG/L
 MASS   =MASS/(0.5*RHO*L**3)
 IZ     =IZ/(0.5*RHO*L**5)
 YRDOT  =-0.00178
 YVDOT  =-0.03430
 YR     =+0.01187
 YV     =-0.03896
 YDRS   =+0.02345
 YDRB   =+0.02345
 NRDOT  =-0.00047
 NVDOT  =-0.00178
 NR     =-0.01022
 NV     =-0.00769
 NDRS   =-0.337*0.02345
 NDRB   =+0.283*0.02345

 DH   =(IZ-NRDOT)*(MASS-YVDOT)-
&     (MASS*XG-YRDOT)*(MASS*XG-NVDOT)
 AA11=((IZ-NRDOT)*YV-(MASS*XG-YRDOT)*NV)/DH
 AA12=((IZ-NRDOT)*(-MASS+YR)-
&     (MASS*XG-YRDOT)*(-MASS*XG+NR))/DH
 AA21=((MASS-YVDOT)*NV-(MASS*XG-NVDOT)*YV)/DH
 AA22=((MASS-YVDOT)*(-MASS*XG+NR)-
&     (MASS*XG-NVDOT)*(-MASS+YR))/DH
 BB11=((IZ-NRDOT)*YDRS-(MASS*XG-YRDOT)*NDRS)/DH
 BB12=((IZ-NRDOT)*YDRB-(MASS*XG-YRDOT)*NDRB)/DH
 BB21=((MASS-YVDOT)*NDRS-(MASS*XG-NVDOT)*YDRS)/DH
 BB22=((MASS-YVDOT)*NDRB-(MASS*XG-NVDOT)*YDRB)/DH

 BB1=BB11+RATIO*BB12
 BB2=BB21+RATIO*BB22

 WRITE (*,*) 'ENTER TC,TL,D'
```

```
OLE=1.0/TC
O1=3.0*POLE
O2=3.0*POLE**2
O3=POLE**3
1=BB1
1=BB2
1=-AD1-(AA11+AA22)
2=(BB1*AA22-BB2*AA12)
2=(BB2*AA11-BB1*AA21)
1=AD3/(BB2*AA11-BB1*AA21)
2=AD2-(AA11*AA22-AA12*AA21)+BB2*K1
2=(C1*B2-C2*B1)/(A1*B2-A2*B1)
3=(C2*A1-C1*A2)/(A1*B2-A2*B1)

IME=100.0
T=0.1
=TIME/DT
Y=TL/DT

SI= 0.0
=   0.0
=   0.0
  = 0.5
  = 0.0
COUNT=0
CON=Y

O 10, I=1,N
 T= T+DT

 PSIDOT=R
 VDOT  =AA11*V + AA12*R + BB1*DEL
 RDOT  =AA21*V + AA22*R + BB2*DEL
 XDOT  =COS(PSI)-V*SIN(PSI)
 YDOT  =SIN(PSI)+V*COS(PSI)

 PSI=PSI+(PSIDOT*DT)
 V=V+(VDOT*DT)
 R=R+(RDOT*DT)
 X=X+(XDOT*DT)
 Y=Y+(YDOT*DT)

 ICOUNT=ICOUNT+1
 IF (ICOUNT.NE.IY) GO TO 11
 YCON=Y
 ICOUNT=0

 PSIC=-ATAN(YCON/D)
 DEL=K1*(PSI-PSIC)+K2*V+K3*R
 DEL=D0*TANH(DEL/D0)

 WRITE(20,*) T,Y
  WRITE(30,*) T,Y
CONTINUE
END
```

APPENDIX C

```
C     PROGRAM THESNEWT.FOR (TWO POINT TIME DELAY ANALYSIS)

       IMPLICIT DOUBLE PRECISION (A-H,O-Z)
       DOUBLE PRECISION K1,K2,K3,L,NR,NV,NDRS,NDRB,IZ,MASS,
      & NRDOT,NVDOT
       DIMENSION A(4,4),FV1(4),IV1(4),ZZZ(4,4),WR(4),WI(4)
       DIMENSION DIST(10,10)
       OPEN (11,FILE='TCN8.DAT',STATUS='NEW')

C     Vehicle Parameters:
       U=     5.0
       RATIO= 0.0
       WEIGHT=435.0
       IZ    =45.0
       L     =7.3
       RHO   =1.94
       G     =32.2
       XG    =0.0104
       MASS  =WEIGHT/G

       YRDOT =-0.00178*0.5*RHO*L**4
       YVDOT =-0.03430*0.5*RHO*L**3
       YR    =+0.01187*0.5*RHO*L**3
       YV    =-0.03896*0.5*RHO*L**2
       YDRS  =+0.02345*0.5*RHO*L**2
       YDRB  =+0.02345*0.5*RHO*L**2
       NRDOT =-0.00047*0.5*RHO*L**5
       NVDOT =-0.00178*0.5*RHO*L**4
       NR    =-0.01022*0.5*RHO*L**4
       NV    =-0.00769*0.5*RHO*L**3
       NDRS  =-0.337*0.02345*0.5*RHO*L**3
       NDRB  =+0.283*0.02345*0.5*RHO*L**3

       DH  =(IZ-NRDOT)*(MASS-YVDOT)-
      &     (MASS*XG-YRDOT)*(MASS*XG-NVDOT)
       AA11=((IZ-NRDOT)*YV-(MASS*XG-YRDOT)*NV)/DH
       AA12=((IZ-NRDOT)*(-MASS+YR)-
      &     (MASS*XG-YRDOT)*(-MASS*XG+NR))/DH
       AA21=((MASS-YVDOT)*NV-(MASS*XG-NVDOT)*YV)/DH
       AA22=((MASS-YVDOT)*(-MASS*XG+NR)-
      &     (MASS*XG-NVDOT)*(-MASS+YR))/DH
       BB11=((IZ-NRDOT)*YDRS-(MASS*XG-YRDOT)*NDRS)/DH
       BB12=((IZ-NRDOT)*YDRB-(MASS*XG-YRDOT)*NDRB)/DH
       BB21=((MASS-YVDOT)*NDRS-(MASS*XG-NVDOT)*YDRS)/DH
       BB22=((MASS-YVDOT)*NDRB-(MASS*XG-NVDOT)*YDRB)/DH

       BB1=BB11+RATIO*BB12
       BB2=BB21+RATIO*BB22

C       WRITE (*,1005)
```

```
READ  (*,*)     TL

RITE (*,1006)
EAD (*,*)     TC

PS=1.D-10
TMAX=100000

L=0.01
O 4 I=1,100
LD = TL * L/U

DO 1 J=1,100
 TCD=TC*L/U
 POLEC=1.0/TCD
 AD1=3.0*POLEC
 AD2=3.0*POLEC**2
 AD3=POLEC**3
 A1=BB1*U*U
 B1=BB2*U*U
 C1=-AD1-(AA11+AA22)*U
 A2=(BB1*AA22-BB2*AA12)*U**3
 B2=(BB2*AA11-BB1*AA21)*U**3
 K1=AD3/((BB2*AA11-BB1*AA21)*U**3)
 C2=AD2-(AA11*AA22-AA12*AA21)*U**2+BB2*U*U*K1
 K2=(C1*B2-C2*B1)/(A1*B2-A2*B1)
 K3=(C2*A1-C1*A2)/(A1*B2-A2*B1)

 A1= (AA11*BB2-AA21*BB1)*U*U*U*K1
 A2= (AA11*AA22-AA12*AA21)*U*U+(AA11*BB2-AA21*BB1)*U*U*U*K3+
     (AA22*BB1-AA12*BB2)*U*U*U*K2-BB2*U*U*K1
 A3=-(AA11+AA22)*U-(BB1*K2+BB2*K3)*U*U
 B0= (AA11*BB2-AA21*BB1)*U*U*U*U*K1
 B1=-(AA12*BB2-AA22*BB1)*U*U*U*K1-BB2*U*U*U*K1
 B2=-BB1*U*U*K1

 AQ=B2*A3-B1
 BQ=B1*A2-B2*A1-B0*A3
 CQ=B0*A1
 DET=BQ**2-4.D0*AQ*CQ
 IF (DET.LT.0.D0) GO TO 4
 ZT1=(-BQ+DSQRT(DET))/(2.0D0*AQ)
 ZT2=(-BQ-DSQRT(DET))/(2.0D0*AQ)
 IF (ZT1.GE.0.D0) OM=DSQRT(ZT1)
 IF (ZT2.GE.0.D0) OM=DSQRT(ZT2)
 ALPHA1=AQ
 ALPHA2=BQ
 ALPHA3=CQ
 BETA1=-B2
 BETA2=B0+B2*A2-B1*A3
 BETA3=B1*A1-B0*A2

 OMOLD=OM

 BETA=BETA1*OMOLD**5+BETA2*OMOLD**3+BETA3*OMOLD
 ALPHA=ALPHA1*OMOLD**4+ALPHA2*OMOLD**2+ALPHA3
 BEP=5.D0*BETA1*OMOLD**4+3.D0*BETA2*OMOLD**2+BETA3
 ALP=4.D0*ALPHA1*OMOLD**3+2.D0*ALPHA2*OMOLD
 F1=BETA*DSIN(2.D0*OMOLD*TLD)-2.D0*BETA*DSIN(OMOLD*TLD)
 F2=ALPHA*DCOS(2.D0*OMOLD*TLD)-2.D0*ALPHA*DCOS(OMOLD*TLD)
```

```
      FP1=BEP*DSIN(2.D0*OMOLD*TLD)+BETA*2.D0*TLD*DCOS(2.D0*OMOLD*TLD)
      FP2=-2.D0*BEP*DSIN(OMOLD*TLD)-2.D0*BETA*TLD*DCOS(OMOLD*TLD)
      FP3=ALP*DCOS(2.D0*OMOLD*TLD)-ALPHA*2.D0*TLD*DSIN(2.D0*OMOLD*TLD)
      FP4=-2.D0*ALP*DCOS(OMOLD*TLD)+2.D0*TLD*ALPHA*DSIN(OMOLD*TLD)
      FPRIME= FP1+FP2+FP3+FP4
      IF (FPRIME.EQ.0.D0) STOP 1112
      IF (F.EQ.0.D0) GO TO 2
      OMNEW=OMOLD-F/FPRIME
      OMDIF=DABS(OMNEW-OMOLD)
      IF (OMDIF.LE.EPS) GO TO 2
      OMOLD=OMNEW
      IT=IT+1
      IF (IT.GT.ITMAX) STOP 1111
      GO TO 3

   2  OM=OMNEW
      XDNUM1=DSQRT((B0-B2*OM**2)**2+(B1*OM)**2)
      XDNUM2=DSQRT((2.D0*DCOS(OM*TLD)-DCOS(2.D0*OM*TLD))**2+
     & (DSIN(2.D0*OM*TLD)-2.D0*DSIN(OM*TLD))**2)
      XDNUM=XDNUM1*XDNUM2
      XDDEN=OM*DSQRT((A1-A3*OM**2)**2+(A2*OM-OM**3)**2)
      XD=XDNUM/XDDEN
      X=XD/L
       DIST(I,J)=X
      WRITE(11,*) X,TL
     TC=TC + 0.015
   1 CONTINUE
    TL=TL + 0.02
   4 CONTINUE
     WRITE(11,20) ((DIST(I,J),J=1,10),I=1,10)
20   FORMAT(10(2X,F4.2))
1005 FORMAT (' ENTER TIME LAG')
1006 FORMAT (' ENTER TIME CONSTANT')
     END
```

LIST OF REFERENCES

1. Bahrke, F., "On Line Identification of the Speed, Steering, and Diving Response Parameters of an Autonomous Underwater Vehicle from Experimental Data", M.E. Thesis, Naval Postgraduate School,Monterey, CA, March, 1992.

2. Chow, S.N. and Mallet, Paret, J., "Integral Averaging and Bifurcation", Journal of Differential Equations, Vol. 26, pp.112-159, 1977.

3. Cottle, D.J., "Mine Avoidance and Localization for Underwater Vehicles Using Continuous Curvature Generation and Non-Linear Tracking Control", M.E. Thesis, Naval Postgraduate School, Monterey, CA, September 1993.

4. Friendland, B., Control System Design: An Introduction to State-Space Methods,McGraw Hill, New York, 1986.

5. Guckenheimer, J. and Holmes, P., Nonlinear Oscillations, Dynamical Systems, and Bifurcations of Vector Fields, Springer Verlag, New York, 1983.

6. Hassard, B. and Wan, Y.H., "Bifurcation Formula Derived from Center Manifold Theory", Journal of Mathematical Analysis and Applications, Vol 63, pp. 297-312, 1978.

7. Healey, A.J., McGhee, R.B., Cristi, R., Papoulias, F.A., Kwak, S.H., Kanayama, Y., Lee, Y., Shukla, S., and Zaky, A., "Research on Autonomous Underwater Vehicles at the Naval Postgraduate School"' Naval Research Reviews, Vol. XLIV, No. 1, 1992.

8. Kanayama, Y. and Hartman, B.I., "Smooth Local Path Planning for Autonomous Vehicles", Proceedings, IEEE International Conference on Robotics and Automation, Scottsdale, Arizona, 1989.

9. Kwak, S.H., McKeon, J.B., Clynch, J.R., and McGhee, R.B., "Incorporation of Global Positioning System into Autonomous Underwater Vehicle Navigation"' Proceedings, IEEE Autonomous Underwater Vehicle Conference, Washington, DC, 1992.

10. Papoulias, F.A., "Bifurcation Analysis of Line of Sight Vehicle Guidance using Sliding Modes", International Journal of Bifurcation and Chaos, Vol. 1, No. 4, 1991.

11. Papoulias, F.A., "Guidance and Control Laws for Vehicle Path Keeping Along Curved Trajectories", Applied Ocean Research, Vol. 14, pp.291-302, 1992.

12. Papoulias, F.A., "Dynamics and Bifurcation of Pursuit Guidance for Vehicle Path Keeping in the Dive Plane"' Journal of Ship Research, Vol. 37, No. 2, 1993.

13. Venne, D.V., "Effects of Positional Information Time Lags on Motion Stability of Autonomous Vehicles", M.S. Thesis, Naval Postgraduate School, Monterey, CA, September, 1992.

INITIAL DISTRIBUTION LIST

		No. Copies
1.	Defense Technical Information Center Cameron Station Alexandria VA 22304-6145	2
2.	Library, Code 052 Naval Postgraduate School Monterey CA 93943-5002	2
3.	Chairman, Code ME Department of Mechanical Engineering Naval Postgraduate School Monterey, CA 93940-5000	1
4.	Program Manager, NA&ME Commandant (G-MTH-2) U.S. Coast Guard 2100 2nd St. SW Washington, DC 20593	1
5.	Mr. Ash Chatterjee Commandant (G-MTH-4) U.S. Coast Guard 2100 2nd St. SW Washington, DC 20593	1
6.	Coast Guard Law Library U.S. Coast Guard 2100 2nd St. SW Washington, DC 20593	1
7.	Naval Engineering Curricular Office, Code 34 Naval Postgraduate School Monterey, CA 93943-5000	1
8.	Professor F. A. Papoulias, Code MEPa Department of Mechanical Engineering Naval Postgraduate School Monterey, CA 93940-5000	4
9.	LCDR George Cummings Commandant (G-MTH-2) U.S. Coast Guard 2100 2nd St. SW Washington, DC 20593	2